 Related Commentary, page 1806

The unique hypusine modification of eIF5A promotes islet β cell inflammation and dysfunction in mice

Bernhard Maier,[1] Takeshi Ogihara,[1] Anthony P. Trace,[2] Sarah A. Tersey,[1] Reiesha D. Robbins,[1,3] Swarup K. Chakrabarti,[4] Craig S. Nunemaker,[5] Natalie D. Stull,[1] Catherine A. Taylor,[6] John E. Thompson,[6,7] Richard S. Dondero,[7] Eli C. Lewis,[8] Charles A. Dinarello,[8] Jerry L. Nadler,[4] and Raghavendra G. Mirmira[1,9]

[1]Department of Pediatrics and Herman B. Wells Center for Pediatric Research, Indiana University School of Medicine, Indianapolis, Indiana, USA. [2]Department of Biochemistry and Molecular Genetics and [3]Department of Pharmacology, University of Virginia, Charlottesville, Virginia, USA. [4]Department of Medicine and Strelitz Diabetes Center, Eastern Virginia Medical School, Norfolk, Virginia, USA. [5]Department of Medicine, University of Virginia, Charlottesville, Virginia, USA. [6]Department of Biology, University of Waterloo, Waterloo, Ontario, Canada. [7]Senesco Technologies Inc., New Brunswick, New Jersey, USA. [8]Department of Medicine, University of Colorado, Aurora, Colorado, USA. [9]Department of Medicine and Department of Cellular and Integrative Physiology, Indiana University School of Medicine, Indianapolis, Indiana, USA.

In both type 1 and type 2 diabetes, pancreatic islet dysfunction results in part from cytokine-mediated inflammation. The ubiquitous eukaryotic translation initiation factor 5A (eIF5A), which is the only protein to contain the amino acid hypusine, contributes to the production of proinflammatory cytokines. We therefore investigated whether eIF5A participates in the inflammatory cascade leading to islet dysfunction during the development of diabetes. As described herein, we found that eIF5A regulates iNOS levels and that eIF5A depletion as well as the inhibition of hypusination protects against glucose intolerance in inflammatory mouse models of diabetes. We observed that following knockdown of eIF5A expression, mice were resistant to β cell loss and the development of hyperglycemia in the low-dose streptozotocin model of diabetes. The depletion of eIF5A led to impaired translation of iNOS-encoding mRNA within the islet. A role for the hypusine residue of eIF5A in islet inflammatory responses was suggested by the observation that inhibition of hypusine synthesis reduced translation of iNOS-encoding mRNA in rodent β cells and human islets and protected mice against the development of glucose intolerance the low-dose streptozotocin model of diabetes. Further analysis revealed that hypusine is required in part for nuclear export of iNOS-encoding mRNA, a process that involved the export protein exportin1. These observations identify the hypusine modification of eIF5A as a potential therapeutic target for preserving islet function under inflammatory conditions.

Introduction

Diabetes is a disorder of glucose homeostasis that afflicts over 200 million people worldwide. Dysfunction or destruction of islet β cells appears to underlie all forms of diabetes. Whereas type 1 diabetes results from the autoimmune destruction of islet β cells, type 2 diabetes is thought to develop as β cell insulin release is unable to compensate for an increasing insulin demand (1). Emerging data suggest that in both forms of diabetes the release of proinflammatory cytokines is central to triggering pathways that initiate β cell dysfunction and eventual death. In the case of type 1 diabetes, a complex interplay between β cells and cells of the immune system leads to the recruitment of activated $CD4^+$ T cells and macrophages into the vicinity of the islet, resulting in local release of proinflammatory cytokines (IL-1β, TNF-α, IFN-γ) (2). In the case of type 2 diabetes, systemic insulin resistance leads to increased circulating proinflammatory cytokines (3), and exogenous administration of IL-1 receptor antagonist (IL-1Ra) has been demonstrated to reduce glycemia and improve β cell function in mice with diet-induced hyperglycemia (4) and in human subjects with type 2 diabetes (5).

Proinflammatory cytokines acutely trigger NF-κB–mediated transcription of the *Nos2* gene encoding iNOS (6). Production of nitric oxide by iNOS contributes to the early pathogenesis of β cell dysfunction in response to cytokines, as nitric oxide inhibits proteins involved in aerobic glycolysis and the electron transport chain, thereby diminishing cellular ATP production (7). This impairment in ATP production limits the coupling of glycolysis to insulin release in the β cell (8). In the longer term, both the iNOS-dependent and -independent effects of cytokine signaling lead to eventual islet death (9–12). Thus, to preserve islet function in the setting of inflammation, it is imperative to identify and counter the mechanisms that mediate islet responsiveness to proinflammatory cytokines.

Eukaryotic translation initiation factor 5A (eIF5A) is a small (17-kDa) protein that is highly conserved throughout evolution (13). eIF5A is the only protein known to contain the unique polyamine-derived amino acid hypusine (N^{ε}-[4-amino-2-hydroxybutyl]-lysine) (14). Hypusine is formed posttranslationally, during a reaction involving residue Lys50 of eIF5A and the sequential action of enzymes deoxyhypusine synthase (DHS) and deoxyhypusine hydroxylase (DOHH), and is necessary for many eIF5A functions (for review see ref. 15).

Authorship note: Bernhard Maier, Takeshi Ogihara, and Anthony P. Trace contributed equally to this study.

Conflict of interest: Charles A. Dinarello is on the Scientific Advisory Board for Senesco Technologies Inc.

Citation for this article: *J Clin Invest.* 2010;120(6):2156–2170. doi:10.1172/JCI38924.

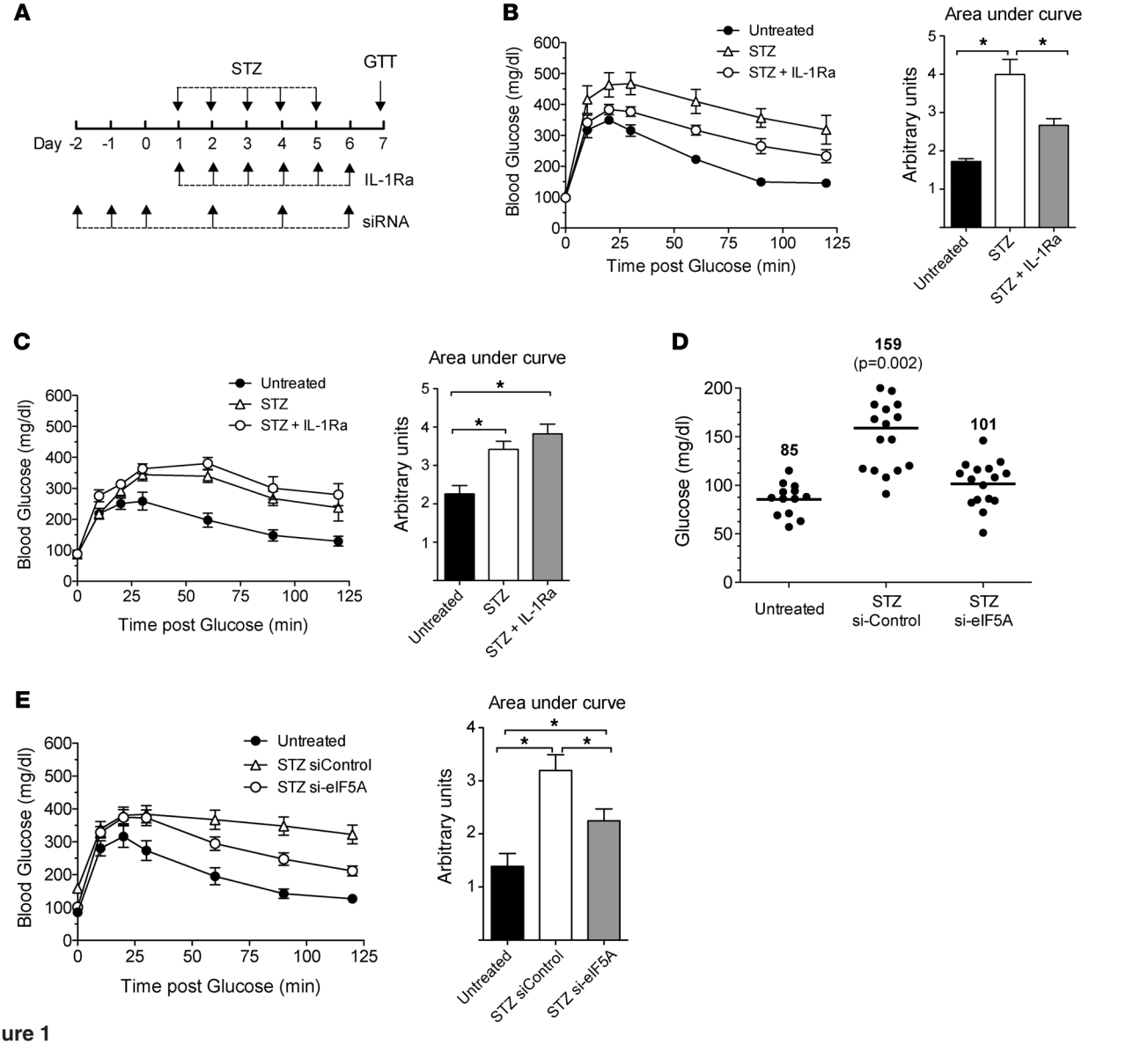

Figure 1

STZ-induced hyperglycemia is partially blocked by IL-1Ra and by knockdown of eIF5A in immunocompetent mice. (**A**) Schematic representation of the STZ, IL-1Ra, and siRNA injection protocol in male mice. (**B**) IPGTTs at day 7 in C57BL/6J male mice ($n = 4$ per group). *$P < 0.05$. (**C**) IPGTTs at day 7 in NOD/SCID/*Il2rg*-null male mice ($n = 4$ per group). *$P < 0.05$. (**D**) Scatter plot of individual fasting blood glucose levels at day 7 in C57BL/6J male mice. The mean fasting blood glucose for si-Control–injected mice is statistically different ($P < 0.05$) compared with untreated mice. Numbers over each set of symbols represent the mean fasting glucose level in mg/dl in each group. Individual symbols represent individual mice, and horizontal bars indicate the mean glucose level for each group. (**E**) IPGTTs at day 7 in C57BL/6J male mice ($n = 13$–17 per group). *$P < 0.05$.

In mammalian cells, eIF5A appears to be a mediator of cellular proliferation (16, 17) and apoptosis (18–20), but its mechanisms have remained vague. The administration of siRNA against eIF5A to mice significantly reduced lethality and production of IL-1, TNF-α, and chemokines in the lungs after endotoxin (LPS) administration (21). Taken together, these studies suggest that eIF5A participates in, and can be essential to, inflammatory responses.

The role of eIF5A in the pathogenesis of islet dysfunction in diabetes has not been directly examined. In the NOD mouse model of type 1 diabetes, approximately 30 distinct chromosomal loci have been identified that appear to contribute to the susceptibility to diabetes (known as insulin-dependent diabetes susceptibility [*Idd*] loci) (22). Interestingly, one of these loci, on the distal arm of chromosome 11 (*Idd4*), harbors genes that are seminal to the autoimmune inflammatory response (e.g., *Il12b*, *Trpv1*, *Nos2*, *Alox15*) (23) and includes the gene encoding eIF5A. In the context of autoimmunity and inflammation, the studies of Hauber and colleagues (24) demonstrated that the hypusinated form of eIF5A (eIF5A^{Hyp}) is essential for the expression of CD83, a cell surface marker that correlates with the maturation of antigen-presenting cells. Thus, eIF5A^{Hyp} appears to be important in the early pathogenesis of the immune response in autoimmune diseases such as type 1 diabetes. However, because pancreatic islets contain eIF5A, we considered the possibility that eIF5A participates in the islet response to autoimmunity

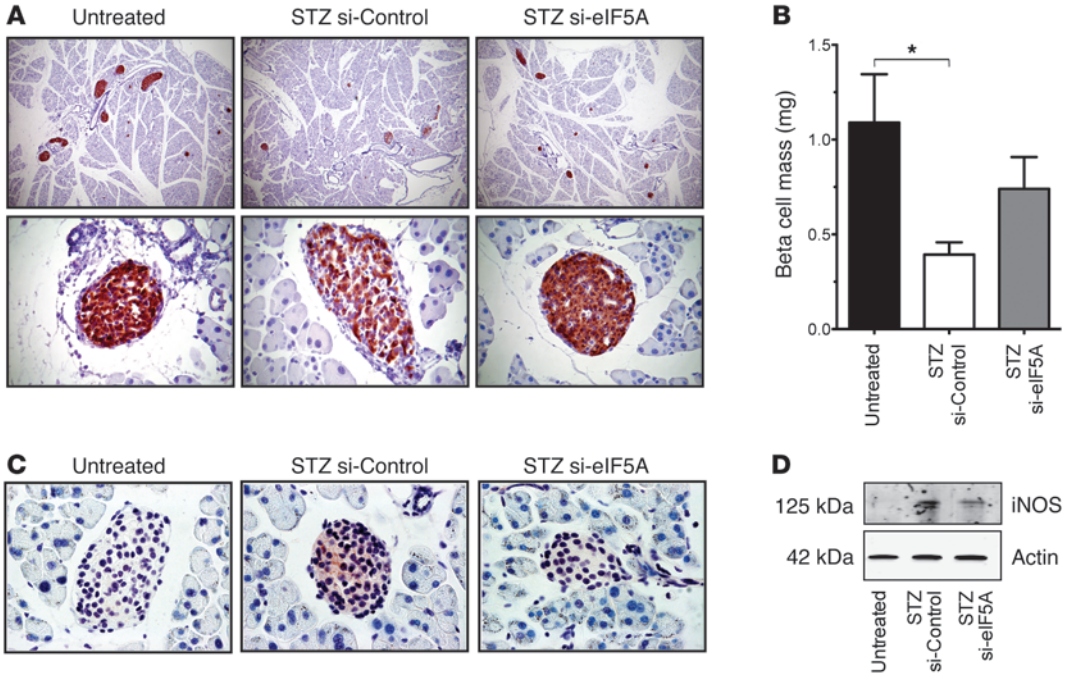

Figure 2

Knockdown of eIF5A in mice preserves islet mass and attenuates iNOS induction following STZ treatment. C57BL/6J male mice were injected with vehicle (untreated) or STZ plus siRNAs, per the protocol in Figure 1A. (**A**) Pancreata from treated mice were sectioned and stained for insulin (red) and counterstained with hematoxylin (blue). Sections from representative pancreata are shown at low (original magnification, ×100; upper panels) and high (original magnification, ×400; bottom panels) magnification. (**B**) β cell mass in treated mice (n = 3 mice per group). *$P < 0.05$. (**C**) At the end of the study, pancreata from treated mice were paraffin-embedded and stained for iNOS (red) and counterstained with hematoxylin (blue). Original magnification, ×630. (**D**) Immunoblots of islet extracts from treated mice following a single dose of STZ. Data are from pooled islets (n = 3 mice per group).

and inflammation. In the present study, we demonstrate that eIF5A^{Hyp} enables cytokine-mediated islet dysfunction through the direct posttranscriptional regulation of the mRNA encoding iNOS (*Nos2*) in both rodent and human cells. Further, we show that depletion of eIF5A or inhibition of hypusination can protect against the development of glucose intolerance in inflammatory mouse models of diabetes. We believe these findings point to a novel pathway in which cytokines are linked to iNOS production via the posttranscriptional regulation of *Nos2* by eIF5A^{Hyp}. These studies therefore identify eIF5A^{Hyp} as a target to mitigate the inflammatory response in pancreatic islets.

Results

Depletion of eIF5A protects mice against multiple low doses of streptozotocin induced hyperglycemia and islet loss. Mammalian eIF5A exists as 2 isoforms, eIF5A1 and eIF5A2, which exhibit differing tissue distributions (25, 26). As shown in Supplemental Figure 1 (supplemental material available online with this article; doi:10.1172/JCI38924DS1), islets and islet-derived cell lines contain only the eIF5A1 isoform, which will henceforth be referred to simply as "eIF5A." To test the role of eIF5A in cytokine-mediated islet dysfunction, we first sought to identify a mouse model of islet inflammation. The multiple low-dose streptozotocin (STZ) model (in which mice are subjected to 5 daily intraperitoneal STZ doses at 55 mg/kg body weight) is considered to provoke local islet inflammation and cytokine release, in part through the recruitment of CD11c$^+$ dendritic cells (27, 28). To demonstrate the dependence of this model on cytokine release from immune cells, we subjected both C57BL/6J mice (with an intact immune system) and NOD/SCID/*Il2rg*-null mice (without innate or adaptive immune systems) to multiple low doses of STZ, as shown in the schematic in Figure 1A. As shown in Figure 1, B and C, both immune-competent (Figure 1B) and -incompetent (Figure 1C) mice exhibit impaired intraperitoneal glucose tolerance tests (IPGTTs) after STZ injections; however, concurrent treatment of mice with IL-1Ra attenuated glucose intolerance only in immune-competent mice. These data suggest that multiple low-dose STZ exhibits at least 2 components contributing to islet dysfunction: one component that is dependent upon cytokine release from immune cells (as observed in C57BL/6J mice) and a second component that involves the known direct toxic, DNA-alkylating effect of STZ (29) (as observed in both C57BL/6J mice and NOD/SCID/*Il2rg*-null mice).

To determine a role for eIF5A during the pathogenesis of islet inflammation in diabetes, we sought to deplete mice of eIF5A using the in vivo RNA interference approach of Moore et al. (21). We injected C57BL/6J mice intraperitoneally with either stabilized siRNA against eIF5A (si-eIF5A) or control siRNA (si-Control) daily for 3 days and then subjected the mice to the multiple low-dose STZ protocol (see schematic in Figure 1A). As shown in Figure 1D, although the mice treated with STZ exhibited higher fasting blood glucose levels following STZ injection compared with untreated mice, the average fasting blood glucose levels of mice injected with si-eIF5A (101 mg/dl) were significantly lower than that of mice

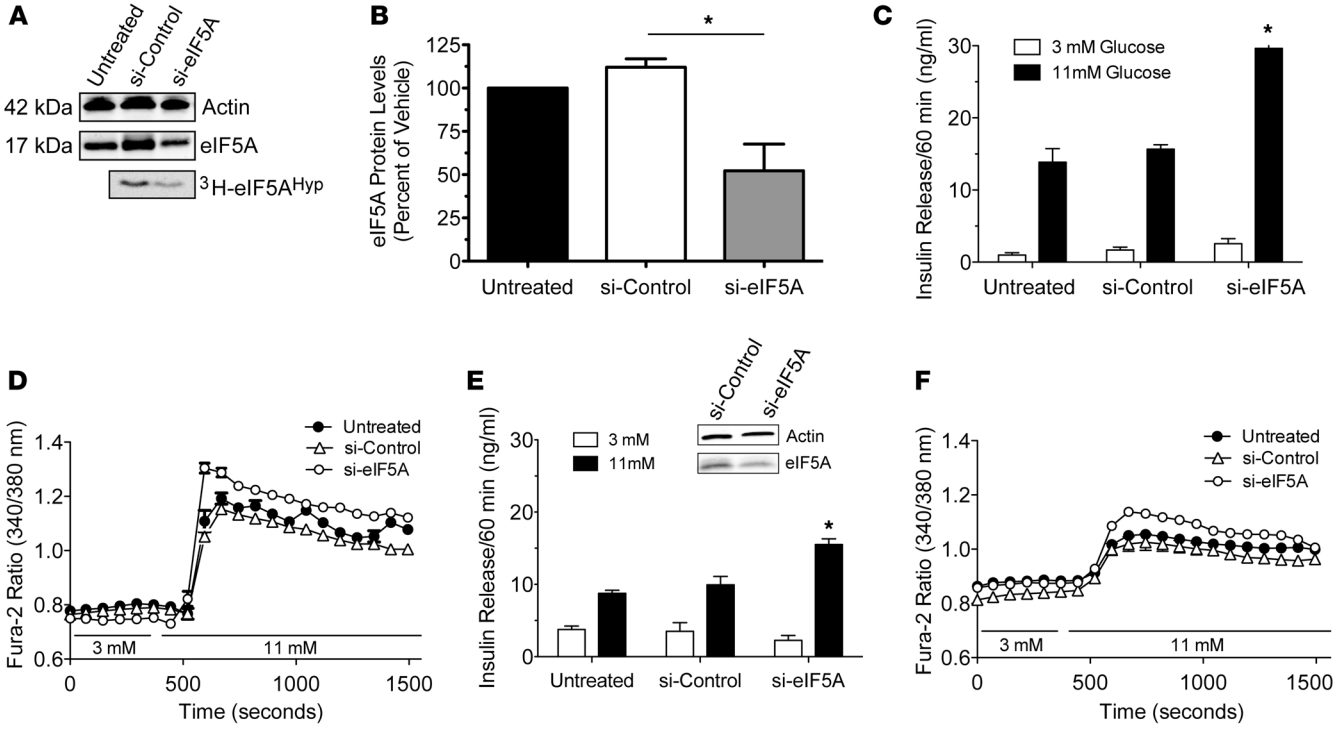

Figure 3

Knockdown of eIF5A causes relative preservation of islet function following cytokine exposure in vitro. Male C57BL/6J mice were injected with vehicle (untreated) or siRNAs as indicated for 3 consecutive days and then euthanized for islet procurement. (**A**) Representative immunoblot of islet extract for actin (top panel) and eIF5A (middle panel). Islets from si-Control– and si-eIF5A–treated animals were pulsed for 4 hours with ^{3}H-spermidine, and then extracts were subjected to electrophoresis and fluorography (bottom panel). (**B**) Quantitation of eIF5A protein levels (normalized to actin protein levels) from islets from injected mice ($n = 3$ per group). *$P < 0.05$. (**C** and **D**) Islets from injected mice were subjected to studies of (**C**) GSIS and (**D**) GSCa at the indicated glucose concentrations. *$P < 0.05$, compared with untreated islets. (**E** and **F**) Islets from injected mice were treated with a cocktail of cytokines (IL-1β, TNF-α, IFN-γ) for 4 hours, and then subjected to (**E**) GSIS and (**F**) GSCa at the indicated glucose concentrations. *$P < 0.05$, compared with untreated islets. The immunoblot in **E** shows islet extract for actin and eIF5A following cytokine exposure. ^{3}H-eIF5A^{Hyp}, tritium-labeled eIF5A.

injected with si-Control (159 mg/dl). Consistent with these fasting blood glucose data, IPGTTs showed that si-eIF5A–treated mice exhibited improved glucose tolerance compared with si-Control–injected mice (Figure 1E).

To determine whether the administration of si-eIF5A affected islet viability following STZ treatment, we next performed immunohistochemical analysis of the pancreata of mice. As shown in Figure 2A, si-Control–injected mice showed an apparent reduction in islet number and weaker insulin staining (i.e., degranulation) relative to mice not given STZ. In contrast, si-eIF5A–injected mice exhibited relatively preserved islet number and insulin granularity. To quantify the differences in islet mass between STZ-treated and untreated animals, we performed morphometry of insulin-stained pancreatic sections. As shown in Figure 2B, si-Control–injected mice exhibited a 2.8-fold reduction of β cell mass compared with non–STZ-treated controls, whereas si-eIF5A–injected animals demonstrated only a statistically insignificant 1.4-fold reduction. These data suggest that eIF5A is required for the early events that lead to eventual islet dysfunction following STZ treatment.

eIF5A mediates cytokine toxicity and iNOS production in islets. As noted earlier, low-dose STZ-induced islet dysfunction involves at least 2 mechanisms: an inflammatory mechanism that is dependent upon cytokine release from immune cells and a direct toxic mechanism on the islet itself. To distinguish whether eIF5A depletion affected one or both of these mechanisms, we performed injections of si-eIF5A in NOD/SCID/*Il2rg*-null mice, which lack fully functional immune cells and therefore react to STZ via direct islet toxicity. Similar to IL-1Ra injections, si-eIF5A injections did not protect against glucose intolerance in NOD/SCID/*Il2rg*-null mice (data not shown), suggesting that eIF5A is involved in only the cytokine-mediated component of STZ-induced islet dysfunction. Because cytokines rapidly induce production of iNOS (30), we expected that si-eIF5A injections should block or attenuate production of iNOS in response to STZ injections in immune-competent mice. As shown in Figure 2C, immunohistochemical staining for iNOS persisted in islets of si-Control–injected animals at the end of the study but was undetectable in si-eIF5A–injected animals. We next isolated and pooled islets from 3 C57BL/6J mice per group, 24 hours after the initial STZ dose, and assessed iNOS content by immunoblot. As shown in Figure 2D, iNOS was rapidly induced in islets within 24 hours of the first STZ treatment in si-Control mice, but this induction was attenuated in si-eIF5A mice. These data support the hypothesis that cytokine-induced iNOS production may underlie the early events of STZ-induced islet dysfunction and loss and that si-eIF5A treatment mitigates iNOS production.

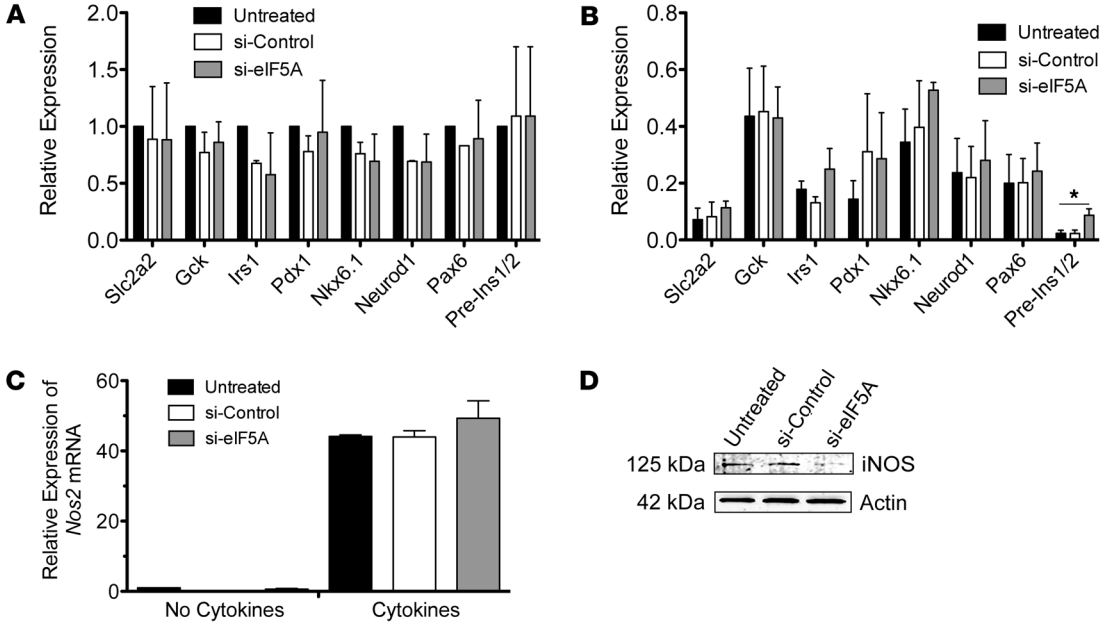

Figure 4

Cytokine signaling to *Nos2* translation is impaired in islets depleted of eIF5A. Male C57BL/6J mice were injected with vehicle (untreated) or siRNAs for 3 consecutive days and then euthanized for islet procurement. (**A**) Islets from injected mice were subjected to quantitative RT-PCR for the genes indicated. Data for each gene were normalized to *Actb* mRNA levels and then reported as expression relative to vehicle (untreated). (**B**) Islets from injected mice were exposed to cytokines for 4 hours and then subjected to quantitative RT-PCR for the genes indicated. Data for each gene were normalized to *Actb* mRNA levels and then reported as expression relative to non–cytokine-treated, vehicle injection. **P* < 0.05. (**C**) Islets from injected mice were untreated or treated with cytokines for 4 hours and then subjected to quantitative RT-PCR for *Nos2* mRNA. Data were normalized to *Actb* mRNA levels and then reported as expression relative to non–cytokine-treated, vehicle injection. (**D**) Representative iNOS and actin immunoblots of islet extracts from injected mice treated with cytokines for 4 hours. (**A**–**C**) Data are from 3 independent islet isolations.

Depletion of eIF5A protects islets from cytokine-induced dysfunction in vitro. Our studies to this point suggest a role for eIF5A in mediating systemic cytokine responses but do not directly implicate its action in pancreatic islets. We therefore isolated islets from siRNA-injected mice and assessed their function in vitro. As shown in Figure 3, A and B, intraperitoneal injection of si-eIF5A for 3 days led to approximately 50% reduction of eIF5A in islets, as determined by immunoblot. Importantly, ^{3}H-spermidine incubations revealed a similar reduction in eIF5A^{Hyp} in islets of si-eIF5A mice (Figure 3A). This depletion corresponded to a significant improvement in islet response to glucose stimulation, as determined by glucose-stimulated insulin secretion (GSIS) studies (Figure 3C). To further characterize this improvement in islet glucose responsiveness, we also performed glucose-stimulated Ca^{2+} mobilization (GSCa) studies. GSCa is a measure of islet glucose sensitivity that captures the dynamics of the islet glucose response, which is similar to GSIS (31). The GSCa, as measured by the change in Fura-2 AM fluorescence ratio after glucose stimulation, was increased in si-eIF5A–treated islets compared with controls, reflecting the functional improvement seen in GSIS (Figure 3D). This improved GSCa, relative to controls, persisted for 48 and 72 hours after isolation (data not shown).

The improvement in islet function following the knockdown of eIF5A suggests that eIF5A may contribute to the stress of collagenase exposure during islet isolation. To directly assess whether eIF5A contributes to stress responses in the islet, we next exposed islets to a cocktail of proinflammatory cytokines (IL-1β, TNF-α, IFN-γ), inducing a condition thought to mimic islet inflammation, as seen in multiple low-dose STZ and the major forms of diabetes (32). We used a short cytokine exposure (4 hours) to assess early impairment in islet function independent of islet cell death. As shown in Figure 3, E and F, islets from all 3 groups (vehicle, si-Control, and si-eIF5A) exhibited some impairment in GSIS and GSCa compared with their non–cytokine-exposed counterparts, while islets from mice treated with si-eIF5A showed significant preservation of GSIS and GSCa compared with controls. The immunoblot in Figure 3E shows that eIF5A levels remained persistently lower in the si-eIF5A group even after cytokine exposure. Importantly, islet viability did not differ significantly among groups in these studies, as determined by ethidium homodimer-1/calcein-AM uptake studies, and no activation of caspase 3 was observed during this short time course (data not shown). These data suggest that eIF5A contributes to acute islet dysfunction in response to proinflammatory cytokines, even prior to overt cell death.

Endogenous eIF5A promotes translation of the mRNA encoding iNOS in primary islets. To understand better the protective effect of eIF5A knockdown in primary islets, we next evaluated the transcriptional response using quantitative RT-PCR of genes known to mediate glucose responsiveness and β cell growth (Figure 4, A and B). Although there was relative preservation of *Ins1*/*Ins2* pre-mRNA levels in si-eIF5A islets exposed to cytokines (consistent with the relative preservation of GSIS in these islets), otherwise there were no significant differences in the transcription of any of the studied genes involved in glucose response (*Slc2a2*, *Gck*), insulin signaling (*Irs1*), or β cell growth/differentiation (*Pdx1*, *Nkx6-1*, *NeuroD1*, *Pax6*). Instead, 2- to 10-fold reductions in the steady-state levels of all of these genes occurred in response to cytokines in all groups.

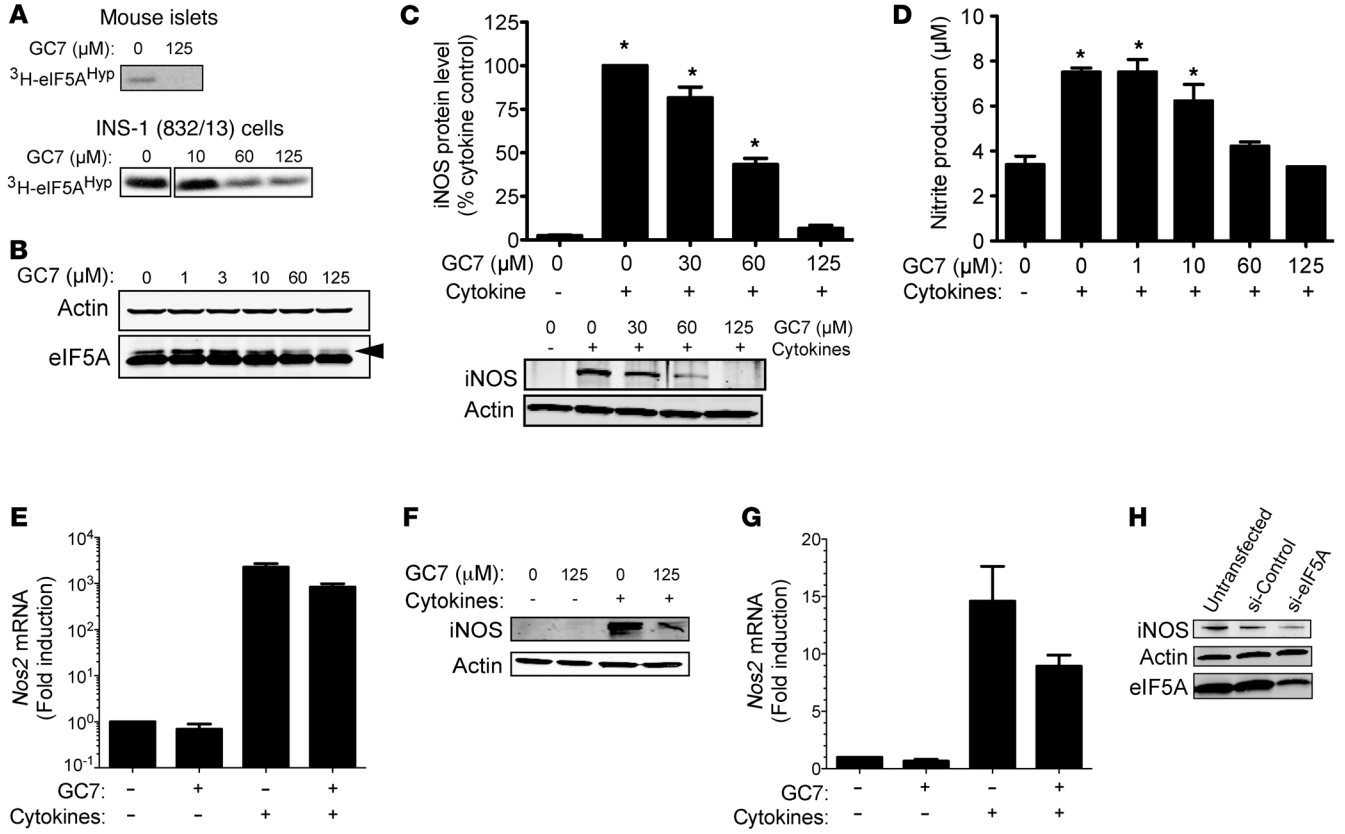

Figure 5

Inhibition of hypusination impairs cytokine-induced *Nos2* translation in INS-1 (832/13) β cells and human islets. (**A**) Mouse islets and INS-1 cells that were treated with GC7 overnight were pulsed with ^{3}H-spermidine for 4 hours and subjected to electrophoresis and fluorography. (**B**) Representative immunoblots of actin and eIF5A from INS-1 cell extracts following overnight treatment with GC7. The arrowhead identifies an upper band of decreasing intensity. (**C**) Representative immunoblot of iNOS and actin from INS-1 cell extracts. The bar graph shows quantitation of iNOS protein levels, normalized to actin levels ($n = 3$). (**D**) Nitrite levels in INS-1 cell medium ($n = 3$). (**C** and **D**) $^*P < 0.05$, compared with the non-cytokine–treated sample. (**E**) *Nos2* transcript levels in INS-1 cells. Data were normalized to *Actb* mRNA levels and are reported as fold induction relative to non-cytokine, non-GC7–treatment. Data are the mean ± SEM from 3 independent experiments. (**F**) Representative immunoblots of iNOS and actin from human islets. (**G**) *Nos2* transcript levels in human islets. Data were normalized to *Actb* mRNA levels and are reported as fold induction relative to non-cytokine, non-GC7–treatment ($n = 3$ experiments from a single human islet donor). (**H**) Representative immunoblots for iNOS, actin, and eIF5A from INS-1 cells transfected with the siRNAs indicated.

Because nitric oxide is a known effector of islet dysfunction following cytokine stress (33), we also examined transcription of the gene encoding iNOS (*Nos2*). As shown in Figure 4C and unlike that of the other genes examined above, we observed a striking 40-fold activation of *Nos2* mRNA in all treatment groups in response to the cytokines. Notably, however, whereas iNOS protein was coordinately induced in islets of mice injected with vehicle or si-Control, induction of iNOS protein was attenuated in islets from si-eIF5A–injected mice (Figure 4D). These data provide evidence that eIF5A may be an important regulator of *Nos2* mRNA translation in primary islets.

Hypusination of eIF5A is essential for Nos2 mRNA translation. eIF5A1 and eIF5A2 are the only proteins known to contain the unique amino acid hypusine at position 50. Hypusine is formed as a post-translational modification of residue Lys50 in a reaction requiring spermidine and catalyzed by the sequential actions of the enzymes DHS and DOHH (34). DHS is the rate limiting enzyme of this biosynthetic pathway, and small molecule inhibitors of this enzyme have been used to specifically inhibit the activity of eIF5A (24, 35). To clarify further the mechanism of eIF5A-regulated translation of *Nos2*, we performed studies following overnight incubation of cells with GC7 (an inhibitor of DHS). As shown in Figure 5A, 125 μM GC7 effectively inhibited new hypusine formation (as determined by ^{3}H-spermidine incorporation) in mouse islets and in the rat cytokine-responsive β cell–derived line INS-1 (832/13) (10). Interestingly, GC7 incubation also depleted the steady-state level of an eIF5A species, as observed by immunoblot (Figure 5B, arrowhead); this latter species may represent a form of eIF5A^{Hyp} akin to that seen in 2D gels and isoelectric focusing (36, 37). Similar to data in primary islets, the immunoblot in Figure 5C (lanes 1 and 2) demonstrates that a 4-hour incubation of INS-1 cells with cytokines resulted in the induction of iNOS. However, incubation with cytokines following increasing concentrations of GC7 resulted in a dose-dependent attenuation of iNOS levels (Figure 5C) as well as nitrite release into the medium (Figure 5D), with the greatest inhibition observed at 125 μM GC7. As with our siRNA studies in islets, the block in iNOS production by GC7 appeared to be at the level of mRNA translation, as *Nos2* transcript levels remained disproportionately elevated, even

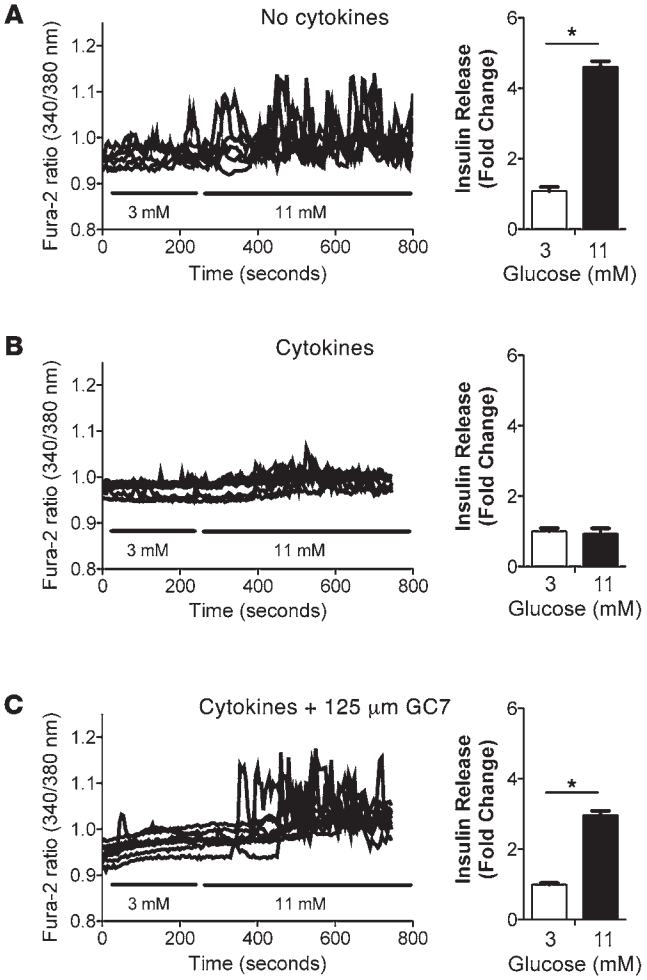

Figure 6
Inhibition of hypusination preserves INS-1 β cell function during cytokine exposure. INS-1 β cells were exposed to (**A**) no treatment, (**B**) 4-hour cytokine incubation, and (**C**) a combination of overnight 125 μM GC7 and 4-hour cytokine incubation and then loaded with Fura-2 dye and subjected to GSCa (left panels) and GSIS studies (right panels) at the indicated glucose concentrations. For the GSCa studies, traces of at least 8 individual cells from a total of 3 independent experiments are shown. GSIS data are from 3 independent experiments. $^*P < 0.05$.

in the presence of 125 μM GC7 (Figure 5E). Similar data using GC7 were obtained in primary mouse islets (data not shown) and in human islets (Figure 5, F and G). To verify that the effect of GC7 was due to inhibition of eIF5A action, we performed siRNA knockdown of eIF5A in INS-1 cells (Figure 5H) and found that cytokine-mediated iNOS induction was indeed attenuated.

Inhibition of hypusination protects against cytokine-induced β cell dysfunction in vitro. To assess INS-1 cell function in the presence of cytokines and GC7, we next performed GSCa and GSIS studies. As shown in Figure 6A (left panel) and unlike that in intact islets, INS-1 cells exhibited an asynchronous GSCa pattern that has been described previously (38); nevertheless, GSCa was closely correlated with GSIS (Figure 6A, right panel). This asynchronous pattern may be referable to the dispersed nature of insulinoma cells compared with β cells in an intact islet. A shown in Figure 6B, GSCa and GSIS were virtually abolished upon incubation with cytokines. Preincubation with 125 μM GC7, however, reversed the suppressive effect of cytokines on GSCa and GSIS almost completely (Figure 6C). Taken together, these results suggest that hypusination of eIF5A is crucial to promoting *Nos2* translation and β cell dysfunction in response to acute exposure to the cytokines.

Short-term GC7 incubations do not affect cellular viability or cell cycle progression. Notably, in the studies described above, concentrations of GC7 in excess of 30 μM were required to substantially block iNOS, raising some concern about the specificity of the drug and possible effects of the drug on cell viability at these concentrations. Because GC7 is known to be inactivated by the action of amine oxidases, which are abundant in serum, typical studies with GC7 in the literature have used aminoguanidine to inhibit amine oxidases (16). When coincubated with 1 mM aminoguanidine, inhibition of new hypusine synthesis was observed at much lower concentrations (along with reductions in the steady-state level of the eIF5A species observed by immunoblot) (Supplemental Figure 2A). Under conditions of aminoguanidine coincubation, inhibition of iNOS could be observed with GC7 concentrations in the 3 μM range (Supplemental Figure 2B). Because aminoguanidine is also an effective inhibitor of iNOS catalytic activity (ref. 39, Supplemental Figure 2C) and can therefore confound interpretation of our data, we elected, in subsequent studies, to forgo use of aminoguanidine and instead use higher concentrations of GC7 (125 μM). At these concentrations, GC7 does not appear to inhibit iNOS activity (Supplemental Figure 2C). To rule out possible adverse effects of GC7 on cell viability, we also performed quantitative 2-color fluorescence analysis of live (calcein-AM–positive) and dead (ethidium homodimer-1–positive) cells using fluorescence cytometry and found that the percentage of dead INS-1 cells (approximately 4%–5%) was unaffected by increasing GC7 concentrations of between 0 to 125 μM after overnight exposure (Supplemental Figure 2D); notably, however, 3-day exposure to 125 μM GC7 or serum starvation led to a dramatic increase in percentage of dead cells (70% and 30%, respectively) (Supplemental Figure 2D). Cell cycle analysis revealed that overnight GC7 treatment (at any concentration) had no significant effect on cell cycle progression (G1-S) in INS-1 cells (Supplemental Figure 2E) or on global translational initiation (as observed by eIF2α phosphorylation; data not shown). Importantly, a cell cycle block was clearly apparent following 3 days of serum depletion or 3 days of GC7 exposure (Supplemental Figure 2E). Long-term, high concentration GC7 treatment has recently been shown to result in impairments in cell cycle progression that are referable to both $eIF5A^{Hyp}$ depletion and interference with polyamine metabolism (37). Taken together, our data verify that our short-term overnight incubations with GC7 do not significantly affect INS-1 cell viability or cell cycle progression.

$eIF5A^{Hyp}$ exhibits a relatively short half-life in islet β cells. The abundance of data in the literature suggests that eIF5A and $eIF5A^{Hyp}$ exhibit prolonged half-lives (>24 hours) in some mammalian cells (40, 41). This prolonged half-life appears seemingly at odds with our relatively rapid inhibition of eIF5A action by overnight GC7 pretreatment and prompted us to assess the half-life of $eIF5A^{Hyp}$ in β cells and islets. As shown in Supplemental Figure 3, pulse-chase experiments using ^{3}H-spermidine revealed that $eIF5A^{Hyp}$ exhibits only approximately 6 hours of half-life in INS-1 β cells and mouse and human islets, whereas a much longer (approximately 15 hours) half-life was seen in HeLa cells. In these pulse-chase experiments, no evidence of cellular death was observed by ethidium homodi-

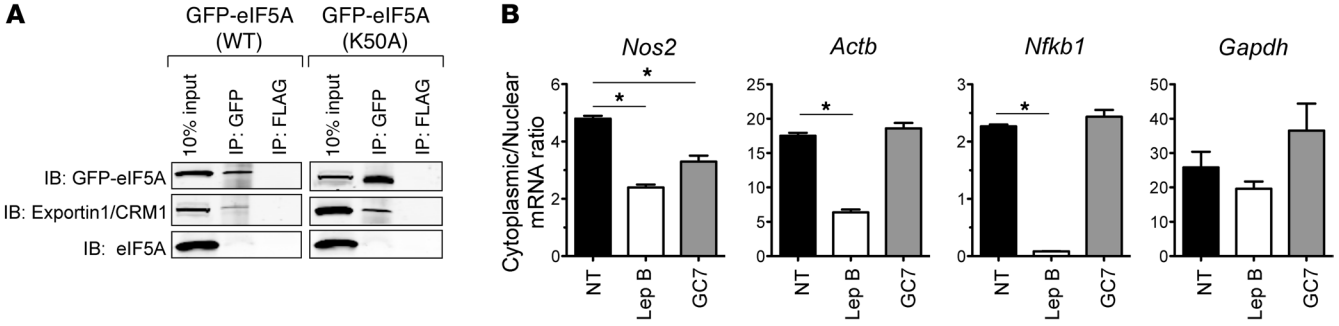

Figure 7

Nos2 mRNA nucleocytoplasmic shuttling in INS-1 β cells is dependent upon exportin1/CRM1 and hypusinated eIF5A. (**A**) INS-1 β cells were transfected with GFP-eIF5A or GFP-eIF5A (K50A) mutant, and cellular extracts were immunoprecipitated with the indicated antibodies and then immunoblotted for GFP, exportin1/CRM1, and eIF5A. (**B**) INS-1 cells were treated for 3 hours with leptomycin B (Lep B), overnight with GC7, or untreated (NT) and then exposed to 4-hour cytokine treatment, followed by fractionation of cytoplasmic and nuclear fractions. RNA from these fractions was subjected to quantitative RT-PCR for *Nos2*, *Actb*, *Nfkb1*, and *Gapdh* mRNAs. Data are expressed as the ratio of mRNA in the cytoplasmic fraction to mRNA in the nuclear fraction ($n = 3$). $^*P < 0.05$.

mer-1/calcein-AM uptake (data not shown). These studies suggest a potentially unique regulation of eIF5A^{Hyp} stability in islet β cells and offer one explanation for the relatively rapid inhibition of eIF5A activity in our GC7 inhibition studies.

eIF5A^{Hyp} is required for nuclear export of Nos2 mRNA. Translational control of mRNA may occur at several levels, including (but not limited to) nuclear export and mRNA cycling between polysomes and P bodies/stress granules (reviewed in ref. 42). Although some controversy exists in the field regarding eIF5A shuttling (e.g., refs. 43 and 44), eIF5A has been shown to interact with the nuclear export proteins exportin1/chromosome region maintenance 1 (exportin1/CRM1) and exportin4 in mammalian cells (45, 46), and we show here its interaction with exportin1/CRM1 in islet β cells (Figure 7A). We therefore performed cellular fractionation studies of cytokine-treated INS-1 cells to determine whether eIF5A is necessary for nuclear export of *Nos2* mRNA. As shown in Figure 7B, *Nos2*, *Actb*, *Nfkb1*, and *Gapdh* mRNAs exhibited a preferentially cytoplasmic distribution in cytokine-treated INS-1 cells. In contrast, preincubation with the exportin1/CRM1 inhibitor leptomycin B caused a relative retention of *Nos2*, *Actb*, and *Nfkb1* (but not *Gapdh*) in the nuclear fraction, suggesting that exportin1/CRM1 serves as a nuclear export protein for these species. Most interestingly, pretreatment of INS-1 cells with GC7 caused relative nuclear retention of *Nos2* mRNA but not of *Actb*, *Nfkb1*, and *Gapdh* mRNAs (Figure 7B), which supports the argument that eIF5A^{Hyp} is required for efficient shuttling of *Nos2* mRNA.

Hypusination and exportin1/CRM1 are required for eIF5A nucleocytoplasmic shuttling. Given the striking retention of *Nos2* transcripts in the absence of eIF5A^{Hyp}, we next asked whether the intracellular distribution of eIF5A accounts for its effect on *Nos2* nucleocytoplasmic shuttling. We therefore performed immunofluorescence of eIF5A in fixed INS-1 cells. As shown in Figure 8A, eIF5A appears to occupy both cytoplasmic and nuclear distributions in quiescent INS-1 cells (but with a slight nuclear predominance). When cells were treated with cytokines, there was a shift in the eIF5A distribution pattern from the nucleus to the cytoplasm. Interestingly, when cells were pretreated with either GC7 or leptomycin B, treatment with the cytokines failed to induce the nuclear-to-cytoplasmic translocation of eIF5A. These data suggest that the nuclear-to-cytoplasmic translocation of eIF5A in response to cytokine stimulation is dependent upon both hypusination and the activity of exportin1/CRM1. To demonstrate that hypusination of Lys50 is required in the nuclear-to-cytoplasmic translocation of eIF5A, we next transfected INS-1 cells with vectors encoding GFP fusions with either wild-type eIF5A or a mutant eIF5A, in which Lys50 is exchanged for Ala (K50A mutant). As shown in Figure 8B, whereas the wild-type fusion protein exhibited nuclear-to-cytoplasmic shuttling upon exposure to cytokines, the localization of the K50A mutant remained unchanged in response to the cytokines. Interestingly, the K50A mutant is still observed to interact with exportin1/CRM1 in coimmunoprecipitation assays (Figure 7A), suggesting the physical association of eIF5A^{Hyp} by itself is not sufficient for nuclear-cytoplasmic shuttling. Taken together, these findings support studies that demonstrate that hypusination causes a shift in eIF5A localization from the nucleus to the cytoplasm in mammalian cells (47, 48).

eIF5A^{Hyp} binds specifically to Nos2 mRNA. The retention of both *Nos2* transcripts and eIF5A in the nucleus upon inhibition of hypusination suggested a close relationship between the 2 molecules, such that eIF5A may serve to chaperone *Nos2* transcripts from the nucleus to the cytoplasm in response to cytokine stimulation. eIF5A^{Hyp} binds to RNAs that contain the consensus sequence 5′-AAAUGU-3′ (49), which is present in the *Nos2* mRNA. To determine whether eIF5A^{Hyp} binds *Nos2* mRNA, we performed RNA immunoprecipitation (RIP) assays using INS-1 cell total RNA. As shown in Figure 9A, cytokine treatment caused induction of a variety of NF-κB target genes, including *Nos2*, *Nfkb1*, *Tnfa*, *Il12a*, and *Il1b*, but not the induction of non–NF-κB targets, including *Il18*, *Il13*, and *Casp3*. Subsequent immunoprecipitation of cytokine-treated INS-1 cells with eIF5A antibody resulted in the coprecipitation of *Nos2* transcripts and 10-fold lower, but statistically significant, coprecipitation of *Nfkb1* transcripts (Figure 9B). In contrast, no coprecipitation of other NF-κB target and nontarget genes were observed. These data document the specificity of mRNA binding by eIF5A^{Hyp}. However, when hypusination is blocked by GC7 no coprecipitation of any mRNA species is observed, suggesting strongly that hypusination of eIF5A is necessary for RNA binding.

GC7 treatment protects mice against STZ-induced hyperglycemia and islet loss. Based on our data thus far, we have reasoned that if hypusination of eIF5A by DHS is required for cytokine responsiveness in islets, then inhibition of DHS in vivo should protect

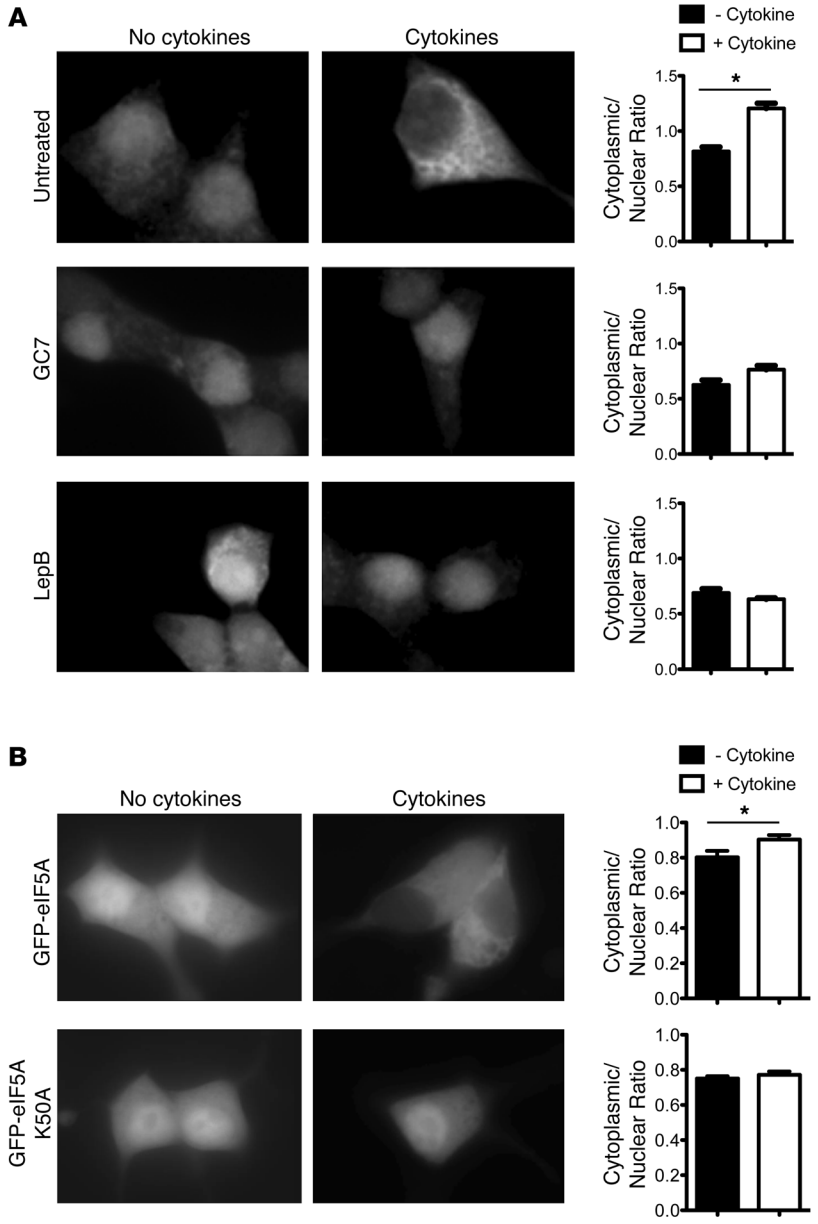

Figure 8
Nucleocytoplasmic shuttling of eIF5A in response to cytokines. (**A**) INS-1 β cells were exposed to vehicle (untreated), GC7 overnight, or leptomycin B for 3 hours and then to 4-hour cytokine treatment (or not) as indicated. Cells were then fixed and stained for eIF5A and visualized by fluorescence microscopy at 488 nm. Representative images are shown. Original magnification, ×630. The cytoplasmic-to-nuclear ratios of eIF5A staining (graphs) were quantitated from cytokine-treated cells and untreated cells exposed to each inhibitor by measurement of spatial pixel intensity. (**B**) INS-1 cells were transfected with expression vectors encoding GFP fusions of either eIF5A or eIF5A (K50A) mutant and then visualized by fluorescence microscopy (488 nm). Representative images are shown. Original magnification, ×630. Quantitation of cytoplasmic-to-nuclear ratios is shown in the graphs. For the ratio graphs, a minimum of 10 cells from 3 different experiments were quantitated. *$P < 0.05$.

against low-dose STZ diabetes. To test this possibility, C57BL/6J mice were treated with GC7 or vehicle and then subjected to low-dose STZ injections. GC7 was delivered in 1 of 2 different ways: either by daily bolus intraperitoneal injections (4 mg/kg/d) or by continuous subcutaneous delivery (40 μg/kg/h) using implanted osmotic pumps. A protocol similar to that shown in Figure 1A was employed in these studies, with GC7 injections or pump implants starting 3 days prior to STZ injections. GC7 treatment, by either intraperitoneal injection (Figure 10A) or osmotic pump (Figure 10B), led to near-complete protection of animals from STZ-induced glucose intolerance. Insulin levels obtained at 0 and 30 minutes during the glucose challenge of pump-implanted animals revealed a defect in insulin secretion in vehicle-treated STZ animals, whereas GC7-treated STZ animals exhibited a normal insulin secretory response (Figure 10C) suggestive of β cell preservation. Histomorphometric analysis of pancreata revealed a trend toward reduced β cell mass in control STZ animals ($P = 0.083$), with full preservation of mass in GC7-injected animals (Figure 10D). As with si-eIF5A treatment, islets of GC7-treated pump animals showed suppression of iNOS production (Figure 10E). Consistent with the known β cell toxic effects of STZ, analysis of pancreatic sections from these animals revealed an increase in β cell TUNEL positivity with STZ treatment, with GC7-treated animals showing fewer $TUNEL^+$ cells per islet (0.42 cells) compared with STZ treatment alone (0.78 cells) (see Supplemental Figure 4). These data therefore suggest that $eIF5A^{Hyp}$ plays an essential role in the early events that lead to islet dysfunction and death in response to inflammation.

$eIF5A^{Hyp}$ promotes islet inflammation independently of the immune system. Because systemic GC7 delivery is expected to inhibit hypusination in all cells that express DHS, it is unclear whether the islet protection afforded by GC7 in vivo is a result of its effects in the islet, the immune cells, or both. As an initial experiment to address this possibility, we assessed the IL-1 responses in STZ-treated C57BL/6J animals by measuring levels of the IL-1–responsive cytokine IL-6. As shown in Figure 10F, whereas concurrent treatment with STZ and IL-1Ra caused a dramatic drop in serum IL-6 levels (consistent with IL-1 inhibition), concurrent treatment with STZ and GC7 did not affect IL-6 levels. No alterations in serum levels of IL-13 and Rantes/CCL5 were observed between treatment groups (Figure 10F). This result suggested that the protection by DHS inhibition was not simply a consequence of inhibiting systemic IL-1 release. To address the role of immune cells more directly, we generated a mouse model to test the role of hypusination in the islet inflammatory response independently of the immune system. LPS is an agent that evokes the NF-κB response through activation of the TLR4 (50), which is also expressed in pancreatic islets (51). Whereas immune-deficient NOD/SCID/*Il2rg*-null mice receiving a single injection of LPS (at 20 mg/kg, a dose that is known to cause

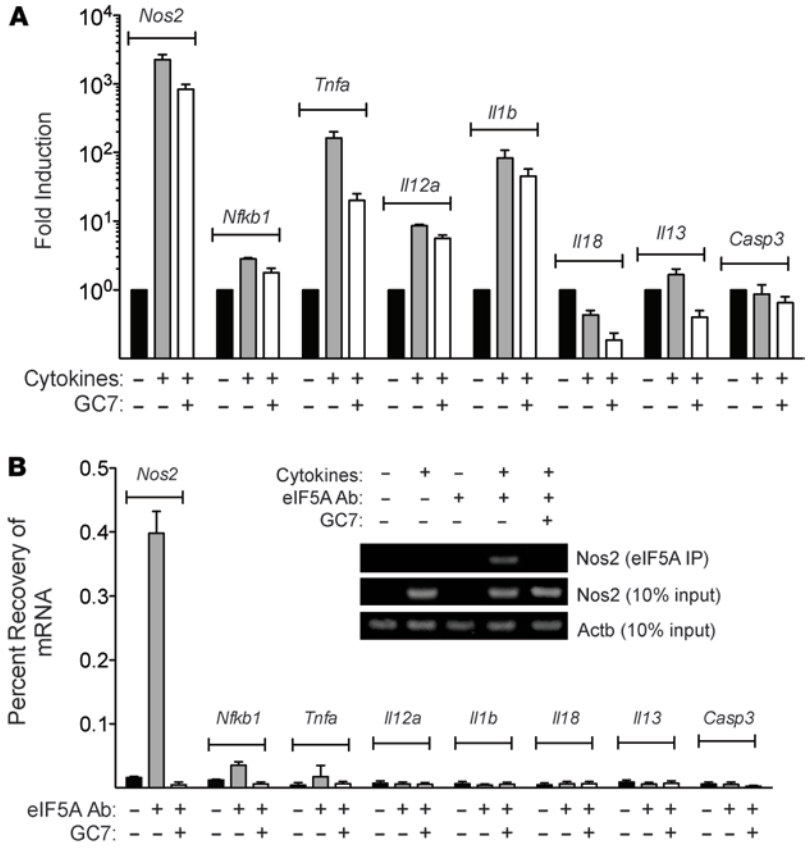

Figure 9
eIF5A specifically interacts with *Nos2* mRNA in INS-1 β cells. (**A**) Quantitative RT-PCR from INS-1 cells exposed to vehicle or GC7 overnight and then to 4-hour vehicle or cytokine treatment as indicated. Data were normalized to *Actb* mRNA and are expressed as fold induction relative to no treatment ($n = 3$). (**B**) RIP assay from INS-1 cells. INS-1 cells were exposed to vehicle or GC7 overnight as indicated and then to 4-hour cytokine treatment. Then, they were subjected to RIP assays using either the eIF5A antibody or an isotype-matched control antibody (FLAG-M2). The bar graph shows quantitative RT-PCR for the genes indicated ($n = 3$). Agarose gel electrophoresis for the genes indicated is shown. Data are expressed as percent recovery relative to input mRNA.

massive inflammatory responses in immune-competent mice; ref. 21) exhibited glucose intolerance and elevated iNOS levels in islets, animals concurrently receiving LPS and GC7 exhibited normal glucose tolerance and attenuated iNOS levels in islets (see Supplemental Figure 5). These data suggest that inhibition of hypusination in vivo can protect islets from iNOS-mediated dysfunction independently of the immune system and further support a role for hypusination within the islet.

Discussion

In both type 1 and type 2 diabetes, a key feature of islet dysfunction is thought to emanate from inflammatory cascades triggered by cytokine signaling. The subsequent production of iNOS and the generation of nitric oxide, among other mediators, has been suggested to cause defects in insulin release (7). In this report, we identify eIF5A^{Hyp} as a proximal regulator of iNOS production and show that eIF5A depletion as well as the inhibition of hypusination preserves islet glucose responsiveness in the presence of cytokine-induced stress. eIF5A, previously known as eIF4D and IF-M2Ba, is a highly conserved 17-kDa protein that was originally characterized as a translation initiation factor, promoting the formation of the first peptide bond in mRNA translation in vitro (52, 53). However, interest in its role in translation initiation has diminished over the years, as studies using yeast mutants show that eIF5A is not essential for general translation but instead probably necessary for the translational elongation of specific transcripts (54). More recently, eIF5A has been thought to function in the translation of mRNAs that encode proteins essential for the G1-S transition of the cell cycle (55), for cytotoxic stress responses (56), and for the propagation of human immunodeficiency virus (57). Thus, eIF5A is best positioned as a factor that controls the balance between cellular proliferation and death, depending upon the nature of cellular stress. The location of the *eIF5A* gene on the distal arm of mouse chromosome 11, within the type 1 diabetes susceptibility locus *Idd4*, and the observation that eIF5A contributes to cytokine responses, led us to speculate that eIF5A may participate in the inflammatory cascade leading to islet death. Whereas eIF5A is expressed in dendritic cells and is necessary for the nuclear-to-cytoplasmic transport of the mRNA encoding the maturation marker CD83, to date no role for eIF5A within the islet has been proposed. We show here that depletion of eIF5A (and its active hypusinated form) in islets using a previously characterized and specific siRNA (21) results in relatively preserved islet glucose responsiveness upon exposure to cytokines, as assessed by GSCa and GSIS. As observed following an approximately 50% decrease in the protein, the phenotype suggests that a nearly full complement of eIF5A^{Hyp} is necessary for the normal stress response to cytokines. To identify the initial pathways leading to islet dysfunction, we intentionally maintained a brief incubation time (4 hours), as more prolonged incubations may lead to convergence of multiple signaling effects, resulting in eventual islet death. Whereas the gene encoding iNOS (*Nos2*) was upregulated in these islets, iNOS protein was strikingly suppressed in si-eIF5A–treated islets compared with controls. These results are consistent with prior reports that *Nos2* transcription and translation can be independently regulated processes (58). Our data show for what we believe is the first time that eIF5A is a factor central to *Nos2* translation.

eIF5A is the only protein known to contain the unique amino acid hypusine (59). Hypusine is formed posttranslationally in a reaction catalyzed by DHS and DOHH and involving transfer of a 4-aminobutyl moiety from spermidine to Lys50 of eIF5A (15). The novelty of this modification in mammalian cells is reflected in the observation that only a single protein (eIF5A1/2) is detectable upon incubation of cells with ^{3}H-spermidine (25). eIF5A and its hypusinated form exhibit prolonged half-lives (≥24 hours) in many mammalian cells (40, 41); strikingly, however, pulse-chase studies revealed that eIF5A^{Hyp} exhibits only approximately 6 hours of half-life in primary islets and islet-derived cell lines (present study). Interestingly, in some cell types, the half-life of eIF5A acutely diminishes to as little as 30 minutes in response

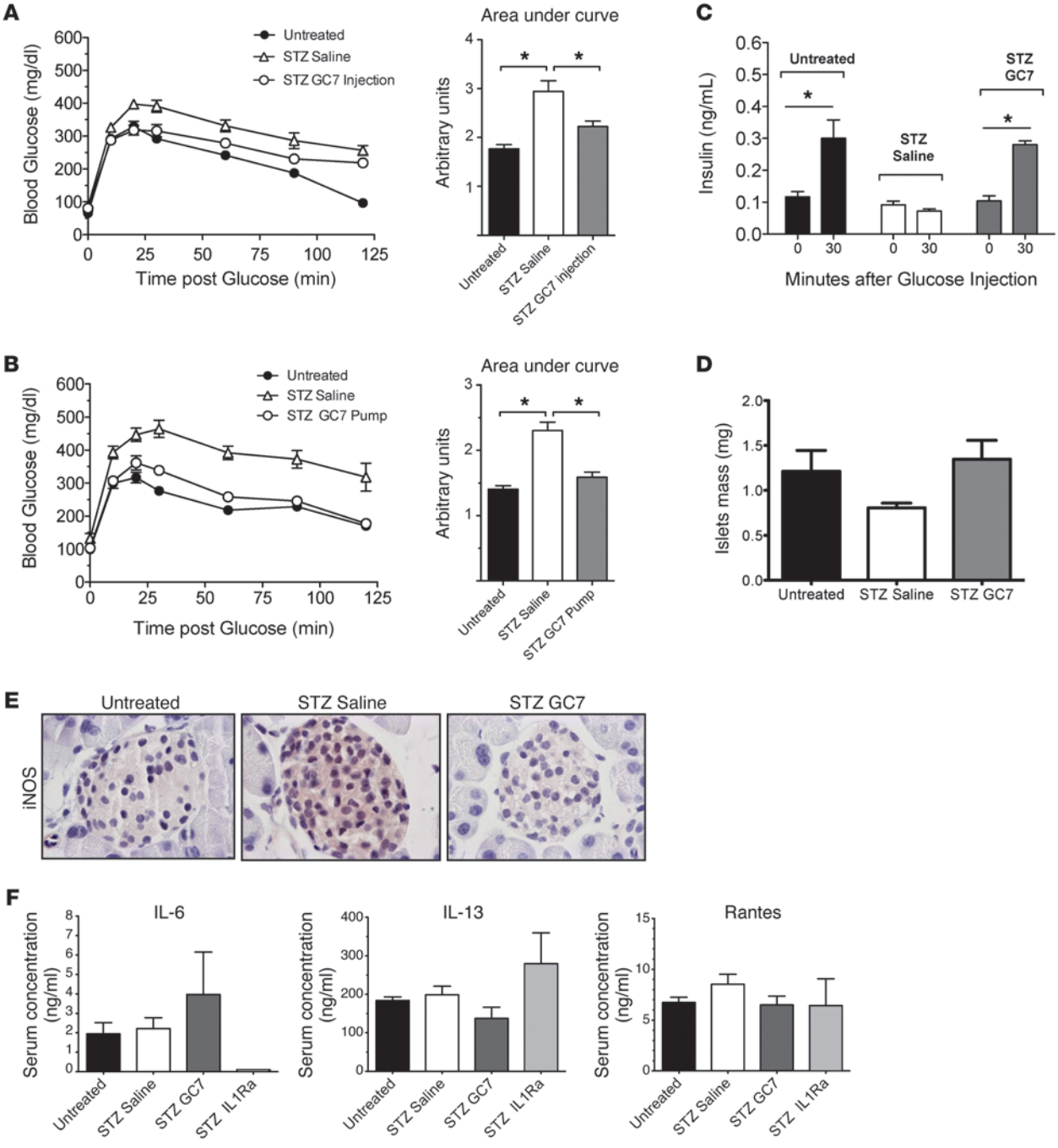

Figure 10

Inhibition of hypusination protects against low-dose STZ-induced hyperglycemia. GC7 or control saline was administered to male C57BL/6J mice by either daily intraperitoneal injection or subcutaneous implanted osmotic pumps. Then, mice underwent 5 consecutive injections of low-dose STZ, as detailed in Figure 1A. (**A** and **B**) IPGTTs at day 7 in mice administered saline or GC7 via (**A**) intraperitoneal injection (n = 6–8) or (**B**) osmotic pump (n = 4). Data are significantly different (*P < 0.05) between all 3 groups in **A** and for STZ saline only in **B**. (**C**) Blood insulin levels at 0 and 30 minutes during the GTT shown in **A** (n = 4). *P < 0.05. (**D**) β cell mass in mice from **A** (n = 3 mice per group). (**E**) Representative images of islets from fixed and stained pancreata from mice in **A** that were stained for iNOS (red) and counterstained with hematoxylin (blue). Original magnification, ×630. (**F**) Serum levels of the indicated cytokines in mice from **A** and from STZ-treated C57BL/6J mice that were intraperitoneally injected with IL-1Ra (see Figure 1B). n = 3–4 animals per group.

to stressors such as heat shock (60, 61), suggesting that both the cell type and environmental conditions can significantly influence the stability of the protein. In our case, therefore, the islet β cell may represent a unique case study for eIF5A^{Hyp} biology.

Upon incubation with an inhibitor to DHS (GC7), we demonstrate that both islets and INS-1 (832/13) β cells exhibit a cytokine-resistant phenotype virtually identical to knockdown of eIF5A protein by siRNA. Whereas islets exhibited a synchronized,

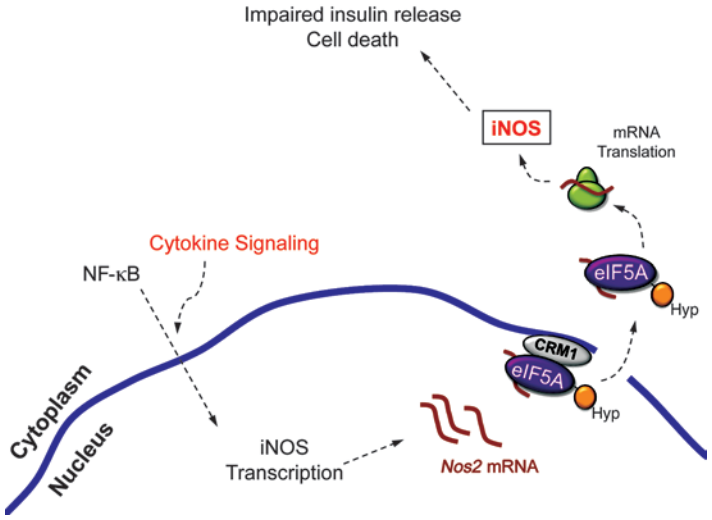

Figure 11
Model for eIF5A control of *Nos2* translation. Signaling from cytokine receptors triggers the nuclear translocation of NF-κB, which activates transcription of the *Nos2* gene. *Nos2* transcripts are shuttled out of the nucleus in a CRM1- and eIF5A-dependent manner, then delivered to ribosomes, where translation occurs to form iNOS. Nitric oxide produced by iNOS leads to suppression of ATP generation and to the eventual inhibition of insulin release. The figure is designed to be descriptive of possible events that are occurring based on data from this and other studies, but it is not meant to be exhaustive or explicit, as many known factors involved in cytokine signaling, eIF5A action, and insulin release have been omitted for clarity. *Hyp*, hypusine.

sigmoidal pattern of Ca^{2+} accumulation in response to glucose, INS-1 cells demonstrated an asynchronous spiking pattern (38) that was effectively abolished upon incubation with cytokines but preserved upon coincubation with GC7. Similar to findings in si-eIF5A–treated islets, incubation with GC7 resulted in a dose-dependent inhibition of iNOS protein levels in INS-1 cells and human islets. Taken together, our studies with DHS inhibition not only support the specificity of the findings using si-eIF5A in islets but also emphasize the importance of hypusination in the action of eIF5A. Hypusination appears to facilitate some protein-protein interactions and also RNA binding by eIF5A (46, 49). With regard to the latter, we identified a potential eIF5A binding sequence within the *Nos2* mRNA and demonstrated that only $eIF5A^{Hyp}$ physically associates with *Nos2* mRNA but significantly less so or not at all with mRNAs for other NF-κB target genes.

To determine how RNA binding might facilitate *Nos2* translation, we considered the possibility that eIF5A aids in the nuclear-to-cytoplasmic transport of *Nos2* mRNA. Nucleocytoplasmic shuttling of eIF5A has been observed by several groups, and the suggestion has emerged that the hypusinated form may be compartmentalized differently from the unhypusinated form (48). Some studies suggest that eIF5A interacts with the nuclear export receptor exportin1/CRM1 and is required for HIV Rev protein-mediated viral RNA export and for the export of *CD83* mRNA in dendritic cells (24, 45, 62, 63). Exportin1/CRM1 serves as a cell context–dependent transporter for certain mRNAs (64), but notably, it mediates (in part) the nucleocytoplasmic transport of *Nos2* (65). In accordance with these studies, we show here that eIF5A forms a physical complex with exportin1/CRM1 in a manner that is not hypusine dependent, and that hypusine is required for the functional export of *Nos2* mRNA in conjunction with exportin1/CRM1. We recognize, however, that the nucleocytoplasmic shuttling of eIF5A has been challenged by other groups (43, 44), and still others purport an interaction between eIF5A and exportin4 (46). We cannot exclude the possibility that exportin4 may also play a role in the transport of *Nos2*, considering that leptomycin B inhibition of exportin1/CRM1 blocked only approximately 50% of *Nos2* export in our hands. Nuclear-cytoplasmic shuttling may not be the only mechanism by which $eIF5A^{Hyp}$ controls *Nos2* translation; although inhibition of hypusination blocked about 50% of *Nos2* nuclear export, more than 90% of iNOS protein production was reduced. This finding implies that $eIF5A^{Hyp}$ is required for linking *Nos2* mRNA to the translational machinery. Prior studies have shown that yeast homolog of eIF5A interacts directly with components of the translational machinery and is necessary for translational elongation (53, 66).

The physiologic relevance of our findings is emphasized by the studies in vivo, which demonstrated that si-eIF5A–injected mice and GC7-treated mice were more resistant to STZ-induced islet dysfunction and hyperglycemia than controls. These studies in vivo closely parallel the results of *Nos2*-null mice, which also showed resistance to STZ and relative islet preservation (30). Although the mechanism of low-dose STZ-induced islet dysfunction and hyperglycemia is complex, many studies point to a toxic effect of STZ on islets, which causes the influx of inflammatory cells with local release of cytokines (27, 28). This mechanism (thought to be similar to that seen in type 1 diabetes) is supported by our findings that the hyperglycemic effect of STZ in immunocompetent mice can be mitigated by the IL-1Ra anakinra. Thus, our findings on the effect of eIF5A in STZ diabetes are similar to those observed upon knockout of other proinflammatory factors residing in the *Idd4* locus, such as 12-lipoxygenase and iNOS (30, 67, 68). Finally, the protective effect of DHS inhibition is borne out in our LPS injection studies in immunodeficient NOD/SCID/*Il2rg*-null mice. These studies support a primary role for DHS and $eIF5A^{Hyp}$ in the inflammatory response within the islet (rather than a secondary effect upon immune cells). We recognize that even in this mouse model, immune cell function (e.g., macrophage activity) may not be completely suppressed, and other cell types (e.g., endothelial cells) may contribute to cytokine production. Therefore, the most definitive evidence for the biology of eIF5A in islets in vivo must await studies of conditional knockouts of eIF5A or DHS.

Taken together, our data identify what we believe to be a novel role for eIF5A and its hypusinating enzyme DHS in effecting the early islet response to cytokine-induced stress. We propose a model (Figure 11) whereby cytokine stimulation collectively leads to rapid induction of *Nos2* gene transcription via activation of the transcription factor NF-κB. This, in turn, leads to the generation of *Nos2* mRNA, which is transported across the nuclear membrane in an exportin1/CRM1-eIF5A–dependent fashion. Possible ongoing binding to eIF5A in the cytoplasm may ensure translation of the transcript at the ribosome. A key component in this model is the hypusination of eIF5A, which is necessary for the binding to *Nos2* transcripts and for the translocation of the complex across the nuclear membrane. Importantly, we recognize that this model is not likely to be exhaustive, with respect

to the phenotypes we observed in vivo. For example, eIF5A^{Hyp} has recently been shown to mediate translational elongation in yeast (53); as such, it is possible that the proinflammatory effects of eIF5A^{Hyp} may be related to regulation of other as yet unidentified transcripts. Nevertheless, our model may clarify prior reports in which treatment of diabetic recipient mice with the DHS inhibitor CNI-1493 led to a more rapid and complete recovery of diabetes following islet transplantation (69). Our studies therefore suggest that targeting of hypusination may represent a novel therapeutic strategy to protect pancreatic islets from inflammation.

Methods

Animals and cells. C57BL/6J mice were purchased from The Jackson Laboratories, and NOD/SCID/*Il2rg*-null mice were bred at the Indiana University Simon Cancer Center. All animal studies were performed under protocols approved by the Indiana University School of Medicine Animal Care and Use Committee or the University of Virginia Animal Care and Use Committee. The cytokine-responsive rat insulinoma cell line INS-1 (832/13) was maintained as previously described (70) and transfected using Metafectene Pro (Biontex), according to manufacturer's instructions. C57BL/6J mouse islets were isolated from collagenase-digested pancreata as described previously (71, 72) and then hand picked and cultured in RPMI medium overnight prior to use. Human islets were obtained commercially (Beta-Pro).

Antibodies and vectors. Polyclonal antibody against eIF5A was from Abcam; monoclonal antibody against eIF5A was from BD Biosciences; monoclonal antibody against eIF5A2 was from Abnova; monoclonal antibody against FLAG-M2 was from Sigma-Aldrich; monoclonal anti-GFP antibody was from Abgent; monoclonal antibody against actin (clone C4) was from MP Biomedicals; and anti-iNOS polyclonal antibody was from Millipore. For immunoblots, fluorophore-labeled secondary antibodies were from Li-Cor (IRDye 800 and IRDye 700). The cDNAs encoding eIF5A1 and eIF5A2 were obtained using PCR cloning from reverse-transcribed human islet RNA and then subcloned into the cytomegalovirus promoter–driven vector pEGFP (Clontech) and verified by automated sequencing. The K50A mutation of eIF5A was generated using oligonucleotide-directed mutagenesis.

siRNA studies. Stabilized siRNAs for intraperitoneal injections were custom synthesized by Dharmacon, using the siSTABLE modification. Groups of 10-week-old C57BL/6J male mice (from The Jackson Laboratories) received daily intraperitoneal injections of 1.6 mg/kg siRNA, prepared in 0.9% saline or vehicle alone (0.9% saline), for 3 days. For in vitro studies, islets from each group of injected mice were harvested on the fourth day and pooled prior to analysis. Injections with each siRNA were performed on at least 3 different occasions. siRNA sequences were as follows: siControl, 5′-AAAGUCGACCUUCAGUAAGGA-3′; si-eIF5A, 5′-AACGGAAUGACUUCCAGCUGA-3′. For siRNA studies in the rat β cell–derived line INS-1 (832/13), cells were transfected with a SMART Pool siRNA against rat eIF5A1 (catalog L-083855-01; Dharmacon) or nontargeting control siRNA #1 (Dharmacon), using DharmaFECT transfection reagent (Dharmacon).

Cytokine and inhibitor incubation studies. For cytokine incubation assays, a 1,000X cocktail of cytokines containing 5 μg/ml IL-1β, 10 μg/ml TNF-α, and 100 μg/ml IFN-γ (all prepared in 0.1% BSA in Tris-buffered saline) was applied at 1X final concentration to groups of 50 islets or 1×10^6 INS-1 (832/13) cells for a total of 4 hours at 37°C. For GC7 incubation studies, GC7 was prepared at a stock concentration of 125 mM in 10 mM acetic acid and applied to cultures of 50 islets or 1×10^6 INS-1 cells to obtain the final concentrations indicted in the figures. Where needed, GC7 was protected from amine oxidases in serum by addition of 1 mM aminoguanidine (Sigma-Aldrich). Cells were incubated with GC7 overnight (approximately 16 hours) at 37°C prior to analysis. Cells were exposed to leptomycin B (Cayman Chemicals) for 3 hours; leptomycin B was prepared at a 1,000X stock concentration of 20 μg/ml in ethanol.

For flow cytometry studies, INS-1 cells (serum starved or pretreated with GC7, as indicated in the figures) were stained with calcein-AM and ethidium homodimer 1 (Live/Dead Kit; Invitrogen) for 30 minutes, and 30,000 cells/sample were analyzed for green (living cells) and red (dead cells) fluorescence, using a FACS Calibur (BD Biosciences) instrument. For cell cycle analysis, 10^6 cells were washed in PBS and fixed in ice-cold 70% ethanol for 1 hour. After washing in PBS, cells were resuspended in Guava cell cycle reagent (Millipore) and incubated at room temperature for 30 minutes. Intercalation of propidium iodide into cellular DNA was quantitated using a FACS Calibur instrument, and the data was analyzed for cell cycle status using Modfit software.

Immunofluorescence. Immunofluorescence of INS-1 cells proceeded essentially as described previously (73), using primary antibodies to eIF5A1 and secondary anti-mouse Alexa Fluor 488–conjugated antibody (Invitrogen) or by direct visualization of GFP fusion proteins at 488 nm. Cells were counterstained with DAPI to visualize nuclei and then imaged using an Axio-Observer Z1 (Zeiss) inverted fluorescent microscope, equipped with an Orca ER CCD camera (Hammamatsu). Quantitation of cytoplasic-to-nuclear ratios of eIF5A staining was performed using Axio-Vision Software, version 4.7 (Zeiss).

Immunostaining and morphometric assessment of β cell mass. Immunostaining of pancreatic sections proceeded as described previously (74). For assessment of islet cell death in pancreatic sections, the technique of TUNEL was performed, using biotinylated 16-dUTP (Roche) and Texas Red Neutravidin (Invitrogen). Digital images were acquired using an Axio-Observer D1 (Zeiss) inverted fluorescence microscope, equipped with a high-resolution color camera. TUNEL-positive/insulin-positive nuclei were counted manually by an observer blinded to sample identity, and data were recoded as the average number of TUNEL-positive nuclei per islet. β cell mass was calculated as described previously (75), but with some modifications. Briefly, pancreata from 3 mice per treatment group were rapidly dissected and weighed, fixed in 4% paraformaldehyde, paraffin-embedded, and longitudinally sectioned. Three sections per pancreas (approximately 75 μm apart) were subsequently immunostained for insulin and counterstained with hematoxylin as described previously (76), and digital images were acquired on an Axio-Observer Z1 microscope (Zeiss) fitted with an AxioCam high resolution color camera. Relative β cell area (calculated using Axio-Vision Software) was multiplied by pancreatic weight to obtain β cell mass. Data represent the average from 3 sections per pancreas, and 3 pancreata from each treatment group.

RIP assays. RIP assays from 1×10^7 formaldehyde cross-linked INS-1 cells were performed as described previously (77). Isotype-matched antibodies against eIF5A and the FLAG-M2 epitope (for control immunoprecipitations) were used at a final dilution of 1:100. Immunoprecipitated RNA was reverse transcribed and subjected to quantitative PCR amplification for selected genes, as described above. All data represent the average of triplicate determinations from at least 3 independent RIP assays.

Immunoblot and nitrite and iNOS assays. Whole cell extracts were resolved by electrophoresis on a 4%–20% SDS-polyacrylamide gel, followed by immunoblot using anti-eIF5A1, anti-eIF5A2, anti-iNOS, anti-GFP, or anti-actin primary antibodies and fluorophore-labeled secondary antibodies. Immunoblots were visualized using the LiCor Odyssey system (LiCor Biosciences) and quantitated by scanning fluorometry using Odyssey Imaging version 3.0 software (LiCor Biosciences). Nitrite was quantitated by measuring nitric oxide–derived nitrite from INS-1 cell culture medium using the Griess reagent (Promega) according to the manufacturer's recommendations. iNOS activity was measured using a commercially available kit (Cayman).

Subcellular fractionation studies. Nuclear and cytoplasmic fractions of 1×10^6 cytokine-treated INS-1 cells exposed to vehicle, leptomycin B (20 ng/ml), or GC7 (100 μM) were prepared using the method described by Dignam et al. (78). Total RNA was isolated from nuclear and cytoplasmic fractions using the RNeasy RNA isolation kit (Qiagen).

Quantitative RT-PCR. Five micrograms of total RNA from islets or INS-1 cells were reverse transcribed, as detailed previously (79). cDNA was subjected to quantitative PCR, using SYBR Green–based technology, and published primers for mouse *Ins1*/*Ins2* pre-mRNA (80) and Quantitech primers (Qiagen) for all other mouse genes (81). The Assay on Demand kit (Applied Biosystems) was used to amplify rat genes in INS-1 cells and human genes in human islets. Thermal cycling was performed according to manufacturer's instructions, and the identity of each PCR product was verified by automated sequencing. All samples were corrected for total input RNA as quantitated by an Experion (Bio-Rad) bioanalyzer. All data represent the average of triplicate determinations from at least 3 independent experiments.

GSCa imaging assays. Intracellular Ca^{2+} was measured using the ratiometric Ca^{2+} indicator Fura-2 AM, as described previously (74). The GSCa was defined as the difference between ratio measurements (340/380 nm fluorescence) in 11 mM versus 3 mM glucose. Data were analyzed with IP Lab software version 4.0 (Scanalytics).

GSIS and IPGTT studies. GSIS and IPGTT studies were performed as described previously (74). Insulin released into the medium was assayed using a 2-site immunospecific ELISA (ALPCO Diagnostics). Glucose was measured using an AlphaTrak glucometer (Abbott). All data represent the average of 3 independent experiments.

Studies in vivo. Daily intraperitoneal STZ injections to groups of 10-week-old C57BL/6J and NOD/SCID/*Il2rg*-null mice occurred at a dose of 55 mg STZ per kg mouse weight for 5 days. GC7 was administered by either daily intraperitoneal injection at a dose of 4 mg/kg mouse weight throughout the duration of the study or by continuous delivery (40 μg/kg/h) via a subcutaneously implanted osmotic pump (Alzet). The IL-1Ra anakinra (50 mg/kg) was given 30 minutes prior to the first dose of STZ, followed by twice daily doses (at 20 mg/kg) until the end of the study. LPS (at a single dose of 20 mg/kg) was given to NOD/SCID/*Il2rg*-null mice by intraperitoneal injection, with or without cotreatment with GC7, as described above. For measurement of serum cytokines, serum was collected via cardiac puncture at the time of euthanasia. Serum was analyzed using a Luminex system (Millipore) and a mouse cytokine/chemokines Panel 1 multiplex kit (Millipore).

Measurement of hypusination. Approximately 100 islets or 1×10^6 INS-1 cells per condition were incubated with 1.5 μCi ^{3}H-spermidine (Perkin Elmer) in the presence of 1 mM aminoguanidine. The measurement of $eIF5A^{Hyp}$ half-life proceeded as described previously (36), with some modification. Briefly, following a 4-hour preincubation with ^{3}H-spermidine, INS-1 cells or islets were incubated with 1 mM spermidine plus 1 mM aminoguanidine for various times and then whole cell extracts were isolated and subjected to electrophoresis on a 12% SDS-polyacrylamide gel. Gels were visualized by fluorography, and bands were quantitated using Kodak Molecular Imaging Software version 5.0 (Kodak).

Statistics. All data are presented as the mean ± SEM. IPGTT statistics were calculated using 1-way repeated measures ANOVA (with Bonferroni post test) and also with area under the curve using the trapezoid method. One-way ANOVA (with Bonferroni post test) was used for comparisons involving more than 2 conditions, and a 2-tailed Student's *t* test was used for comparisons involving 2 conditions. GraphPad Prism (version 5.0) software was used for all statistical analyses. *P* values of less than 0.05 were considered significant.

Acknowledgments

This work is supported in part by grants R01 DK60581 and DK60581-S1 (to R.G. Mirmira), F31 DK079420 (to R.D. Robbins), R01 AI15614 (to C.A. Dinarello), and R01 DK055240 (to J.L. Nadler) from the National Institutes of Health; an investigator-initiated grant from Senesco Technologies Inc. (to R.G. Mirmira); and support from the Ball Brothers Foundation (to R.G. Mirmira). We also wish to acknowledge M. Ryu and B. Tersey for assistance in mouse islet isolation and R. Malik for help with generating eIF5A mutations.

Received for publication December 18, 2009, and accepted in revised form March 10, 2010.

Address correspondence to: Raghavendra G. Mirmira, Indiana University School of Medicine, 635 Barnhill Drive, MS2031, Indianapolis, Indiana 46202, USA. Phone: 317.274.4145; Fax: 317.274.4107; E-mail: rmirmira@iupui.edu.

1. Prentki M, Nolan CJ. Islet beta cell failure in type 2 diabetes. *J Clin Invest*. 2006;116(7):1802–1812.
2. Mathis D, Vence L, Benoist C. beta-Cell death during progression to diabetes. *Nature*. 2001; 414(6865):792–798.
3. Spranger J, et al. Inflammatory cytokines and the risk to develop type 2 diabetes: results of the prospective population-based European Prospective Investigation into Cancer and Nutrition (EPIC)-Potsdam Study. *Diabetes*. 2003;52(3):812–817.
4. Sauter NS, Schulthess FT, Galasso R, Castellani LW, Maedler K. The antiinflammatory cytokine interleukin-1 receptor antagonist protects from high-fat diet-induced hyperglycemia. *Endocrinology*. 2008;149(5):2208–2218.
5. Larsen CM. Interleukin-1-receptor antagonist in type 2 diabetes mellitus. *N Engl J Med*. 2007; 356(15):1517–1526.
6. Eizirik DL, Mandrup-Poulsen T. A choice of death--the signal-transduction of immune-mediated beta-cell apoptosis. *Diabetologia*. 2001;44(12):2115–2133.
7. Leist M, et al. Inhibition of mitochondrial ATP generation by nitric oxide switches apoptosis to necrosis. *Exp Cell Res*. 1999;249(2):396–403.
8. Koster JC, Marshall BA, Ensor N, Corbett JA, Nichols CG. Targeted overactivity of beta cell K(ATP) channels induces profound neonatal diabetes. *Cell*. 2000;100(6):645–654.
9. Chambers KT, Unverferth JA, Weber SM, Wek RC, Urano F, Corbett JA. The role of nitric oxide and the unfolded protein response in cytokine-induced beta-cell death. *Diabetes*. 2008;57(1):124–132.
10. Collier JJ, Fueger PT, Hohmeier HE, Newgard CB. Pro- and antiapoptotic proteins regulate apoptosis but do not protect against cytokine-mediated cytotoxicity in rat islets and beta-cell lines. *Diabetes*. 2006;55(5):1398–1406.
11. Larsen L, et al. Inhibition of histone deacetylases prevents cytokine-induced toxicity in beta cells. *Diabetologia*. 2007;50(4):779–789.
12. Steer SA, Scarim AL, Chambers KT, Corbett JA. Interleukin-1 stimulates beta-cell necrosis and release of the immunological adjuvant HMGB1. *PLoS Med*. 2006;3(2):e17.
13. Facchiano AM, et al. Homology modelling of the human eukaryotic initiation factor 5A (eIF-5A). *Protein Eng*. 2001;14(11):881–890.
14. Cooper HL, Park MH, Folk JE, Safer B, Braverman R. Identification of the hypusine-containing protein hy+ as translation initiation factor eIF-4D. *Proc Natl Acad Sci U S A*. 1983;80(7):1854–1857.
15. Park MH, Nishimura K, Zanelli CF, Valentini SR. Functional significance of eIF5A and its hypusine modification in eukaryotes. *Amino Acids*. 2010; 38(2):491–500.
16. Park MH, Wolff EC, Lee YB, Folk JE. Antiproliferative effects of inhibitors of deoxyhypusine synthase. Inhibition of growth of Chinese hamster ovary cells by guanyl diamines. *J Biol Chem*. 1994;269(45):27827–27832.
17. Caraglia M, et al. The eukaryotic initiation factor 5A is involved in the regulation of proliferation and apoptosis induced by interferon-alpha and EGF in human cancer cells. *J Biochem*. 2003;133(6):757–765.
18. Taylor CA, et al. Role of eIF5A in TNF-alpha-mediated apoptosis of lamina cribrosa cells. *Invest Ophthalmol Vis Sci*. 2004;45(10):3568–3576.
19. Taylor CA, et al. Eukaryotic translation initiation factor 5A induces apoptosis in colon cancer cells and associates with the nucleus in response to tumour necrosis factor alpha signalling. *Exp Cell Res*. 2007;313(3):437–449.
20. Li AL, et al. A novel eIF5A complex functions as a regulator of p53 and p53-dependent apoptosis. *J Biol Chem*. 2004;279(47):49251–49258.
21. Moore CC, et al. Eukaryotic translation initiation factor 5a small interference rna-liposome complexes reduce inflammation and increase survival in murine models of severe sepsis and acute lung injury. *J Infect Dis*. 2008;198(9):1407–1414.
22. Maier LM, Wicker LS. Genetic susceptibility to type 1 diabetes. *Curr Opin Immunol*. 2005;17(6):601–608.
23. Grattan M, Mi QS, Meagher C, Delovitch TL. Congenic mapping of the diabetogenic locus Idd4 to a 5.2-cM region of chromosome 11 in NOD mice: identification of two potential candidate subloci. *Diabetes*. 2002;51(1):215–223.
24. Kruse M, et al. Inhibition of CD83 cell surface expression during dendritic cell maturation by interference with nuclear export of CD83 mRNA. *J Exp Med*. 2000;191(9):1581–1590.
25. Clement PM, Johansson HE, Wolff EC, Park MH. Differential expression of eIF5A-1 and eIF5A-2 in

human cancer cells. *FEBS J*. 2006;273(6):1102–1114.
26. Jenkins ZA, Haag PG, Johansson HE. Human eIF5A2 on chromosome 3q25-q27 is a phylogenetically conserved vertebrate variant of eukaryotic translation initiation factor 5A with tissue-specific expression. *Genomics*. 2001;71(1):101–109.
27. Lukic ML, Stosic-Grujicic S, Shahin A. Effector mechanisms in low–dose streptozotocin–induced diabetes. *Dev Immunol*. 1998;6(1-2):119–128.
28. Calderon B, Suri A, Miller MJ, Unanue ER. Dendritic cells in islets of Langerhans constitutively present beta cell-derived peptides bound to their class II MHC molecules. *Proc Natl Acad Sci U S A*. 2008;105(16):6121–6126.
29. Lenzen S. The mechanisms of alloxan- and streptozotocin-induced diabetes. *Diabetologia*. 2008;51(2):216–226.
30. Flodstrom M, Tyrberg B, Eizirik DL, Sandler S. Reduced sensitivity of inducible nitric oxide synthase-deficient mice to multiple low-dose streptozotocin-induced diabetes. *Diabetes*. 1999;48(4):706–713.
31. Henquin JC, Nenquin M, Stiernet P, Ahren B. In vivo and in vitro glucose-induced biphasic insulin secretion in the mouse: pattern and role of cytoplasmic Ca2+ and amplification signals in beta-cells. *Diabetes*. 2006;55(2):441–451.
32. Kolb H, Mandrup-Poulsen T. An immune origin of type 2 diabetes? *Diabetologia*. 2005;48(6):1038–1050.
33. Corbett JA, McDaniel ML. Intraislet release of interleukin 1 inhibits beta cell function by inducing beta cell expression of inducible nitric oxide synthase. *J Exp Med*. 1995;181(2):559–568.
34. Chen KY, Liu AY. Biochemistry and function of hypusine formation on eukaryotic initiation factor 5A. *Biol Signals*. 1997;6(3):105–109.
35. Dong Z, et al. Modulation of differentiation-related gene 1 expression by cell cycle blocker mimosine, revealed by proteomic analysis. *Mol Cell Proteomics*. 2005;4(7):993–1001.
36. Nishimura K, Murozumi K, Shirahata A, Park MH, Kashiwagi K, Igarashi K. Independent roles of eIF5A and polyamines in cell proliferation. *Biochem J*. 2005;385(pt 3):779–785.
37. Landau G, Bercovich Z, Park MH, Kahana C. The role of polyamines in supporting growth of mammalian cells is mediated through their requirement for translation initiation and elongation. *J Biol Chem*. 2010;285(17):12474–12481.
38. Herbst M, Sasse P, Greger R, Yu H, Hescheler J, Ullrich S. Membrane potential dependent modulations of calcium oscillations in insulin-secreting INS-1 cells. *Cell Calcium*. 2002;31(3):115–126.
39. Corbett JA, McDaniel ML. The use of aminoguanidine, a selective inos inhibitor, to evaluate the role of nitric oxide in the development of autoimmune diabetes. *Methods*. 1996;10(1):21–30.
40. Duncan RF, Hershey JW. Changes in eIF-4D hypusine modification or abundance are not correlated with translational repression in HeLa cells. *J Biol Chem*. 1986;261(27):12903–12906.
41. Gerner EW, Mamont PS, Bernhardt A, Siat M. Post-translational modification of the protein-synthesis initiation factor eIF-4D by spermidine in rat hepatoma cells. *Biochem J*. 1986;239(2):379–386.
42. Parker R, Sheth U. P bodies and the control of mRNA translation and degradation. *Mol Cell*. 2007; 2007;25(5):635–646.
43. Jao DL, Yu Chen K. Subcellular localization of the hypusine-containing eukaryotic initiation factor 5A by immunofluorescent staining and green fluorescent protein tagging. *J Cell Biochem*. 2002;86(3):590–600.
44. Shi XP, Yin KC, Zimolo ZA, Stern AM, Waxman L. The subcellular distribution of eukaryotic translation initiation factor, eIF-5A, in cultured cells. *Exp Cell Res*. 1996;225(2):348–356.
45. Rosorius O, Reichart B, Kratzer F, Heger P, Dabauvalle MC, Hauber J. Nuclear pore localization and nucleocytoplasmic transport of eIF-5A: evidence for direct interaction with the export receptor CRM1. *J Cell Sci*. 1999;112(pt 14):2369–2380.
46. Lipowsky G, et al. Exportin 4: a mediator of a novel nuclear export pathway in higher eukaryotes. *EMBO J*. 2000;19(16):4362–4371.
47. Jin BF, et al. Proteomic analysis of ubiquitin-proteasome effects: insight into the function of eukaryotic initiation factor 5A. *Oncogene*. 2003;22(31):4819–4830.
48. Lee SB, Park JH, Kaevel J, Sramkova M, Weigert R, Park MH. The effect of hypusine modification on the intracellular localization of eIF5A. *Biochem Biophys Res Commun*. 2009;383(4):497–502.
49. Xu A, Chen KY. Hypusine is required for a sequence-specific interaction of eukaryotic initiation factor 5A with postsystematic evolution of ligands by exponential enrichment RNA. *J Biol Chem*. 2001;276(4):2555–2561.
50. Chow JC, Young DW, Golenbock DT, Christ WJ, Gusovsky F. Toll-like receptor-4 mediates lipopolysaccharide-induced signal transduction. *J Biol Chem*. 1999;274(16):10689–10692.
51. Schulthess FT, et al. CXCL10 impairs beta cell function and viability in diabetes through TLR4 signaling. *Cell Metab*. 2009;9(2):125–139.
52. Kemper WM, Berry KW, Merrick WC. Purification and properties of rabbit reticulocyte protein synthesis initiation factors M2Balpha and M2Bbeta. *J Biol Chem*. 1976;251(18):5551–5557.
53. Saini P, Eyler DE, Green R, Dever TE. Hypusine-containing protein eIF5A promotes translation elongation. *Nature*. 2009;459(7243):118–121.
54. Kang HA, Hershey JW. Effect of initiation factor eIF-5A depletion on protein synthesis and proliferation of Saccharomyces cerevisiae. *J Biol Chem*. 1994;269(6):3934–3940.
55. Chatterjee I, Gross SR, Kinzy TG, Chen KY. Rapid depletion of mutant eukaryotic initiation factor 5A at restrictive temperature reveals connections to actin cytoskeleton and cell cycle progression. *Mol Genet Genomics*. 2006;275(3):264–276.
56. Rahman-Roblick R, et al. p53 targets identified by protein expression profiling. *Proc Natl Acad Sci U S A*. 2007;104(13):5401–5406.
57. Bevec D, et al. Inhibition of HIV-1 replication in lymphocytes by mutants of the Rev cofactor eIF-5A. *Science*. 1996;271(5257):1858–1860.
58. Kroncke KD, Fehsel K, Suschek C, Kolb-Bachofen V. Inducible nitric oxide synthase-derived nitric oxide in gene regulation, cell death and cell survival. *Int Immunopharmacol*. 2001;1(8):1407–1420.
59. Park MH. The post-translational synthesis of a polyamine-derived amino acid, hypusine, in the eukaryotic translation initiation factor 5A (eIF5A). *J Biochem*. 2006;139(2):161–169.
60. Gosslau A, Jao DL, Butler R, Liu AY, Chen KY. Thermal killing of human colon cancer cells is associated with the loss of eukaryotic initiation factor 5A. *J Cell Physiol*. 2009;219(2):485–493.
61. Takeuchi K, Nakamura K, Fujimoto M, Kaino S, Kondoh S, Okita K. Heat stress-induced loss of eukaryotic initiation factor 5A (eIF-5A) in a human pancreatic cancer cell line, MIA PaCa-2, analyzed by two-dimensional gel electrophoresis. *Electrophoresis*. 2002;23(4):662–669.
62. Elfgang C, Rosorius O, Hofer L, Jaksche H, Hauber J, Bevec D. Evidence for specific nucleocytoplasmic transport pathways used by leucine-rich nuclear export signals. *Proc Natl Acad Sci U S A*. 1999;96(11):6229–6234.
63. Hofmann W, et al. Cofactor requirements for nuclear export of Rev response element (RRE)- and constitutive transport element (CTE)-containing retroviral RNAs. An unexpected role for actin. *J Cell Biol*. 2001;152(5):895–910.
64. Schutz S, Chemnitz J, Spillner C, Frohme M, Hauber J, Kehlenbach RH. Stimulated expression of mRNAs in activated T cells depends on a functional CRM1 nuclear export pathway. *J Mol Biol*. 2006;358(4):997–1009.
65. Jang BC, et al. Leptomycin B, a metabolite of Streptomyces, inhibits the expression of inducible nitric oxide synthase in BV2 microglial cells. *Int J Oncol*. 2006;29(6):1509–1515.
66. Zanelli CF, et al. eIF5A binds to translational machinery components and affects translation in yeast. *Biochem Biophys Res Commun*. 2006;348(4):1358–1366.
67. Bleich D, Chen S, Zipser B, Sun D, Funk CD, Nadler JL. Resistance to type 1 diabetes induction in 12-lipoxygenase knockout mice. *J Clin Invest*. 1999;103(10):1431–1436.
68. McDuffie M, et al. Nonobese diabetic (NOD) mice congenic for a targeted deletion of 12/15-lipoxygenase are protected from autoimmune diabetes. *Diabetes*. 2008;57(1):199–208.
69. Hyon SH, Tracey KJ, Kaufman DB. Specific inhibition of macrophage-derived proinflammatory cytokine synthesis with a tetravalent guanylhydrazone CNI-1493 accelerates early islet graft function posttransplant. *Transplant Proc*. 1998;30(2):409–410.
70. Hohmeier HE, Mulder H, Chen G, Henkel-Rieger R, Prentki M, Newgard CB. Isolation of INS-1-derived cell lines with robust ATP-sensitive K+ channel-dependent and -independent glucose-stimulated insulin secretion. *Diabetes*. 2000;49(3):424–430.
71. Gotoh M, Ohzato H, Porter J, Maki T, Monaco AP. Crucial role of pancreatic ductal collagenase injection for isolation of pancreatic islets. *Horm Metab Res Suppl*. 1990;25:10–16.
72. Yang Z, Chen M, Ellett JD, Fialkow LB, Carter JD, Nadler JL. The novel anti-inflammatory agent lisofylline prevents autoimmune diabetic recurrence after islet transplantation. *Transplantation*. 2004;77(1):55–60.
73. Parreiras-E-Silva LT, Gomes MD, Oliveira EB, Costa-Neto CM. The N-terminal region of eukaryotic translation initiation factor 5A signals to nuclear localization of the protein. *Biochem Biophys Res Commun*. 2007;362(2):393–398.
74. Evans-Molina C, et al. PPAR-{gamma} activation restores islet function in diabetic mice through reduction of er stress and maintenance of euchromatin structure. *Mol Cell Biol*. 2009;29(8):2053–2067.
75. Kulkarni RN, Jhala US, Winnay JN, Krajewski S, Montminy M, Kahn CR. PDX-1 haploinsufficiency limits the compensatory islet hyperplasia that occurs in response to insulin resistance. *J Clin Invest*. 2004;114(6):828–836.
76. Francis J, Chakrabarti SK, Garmey JC, Mirmira RG. Pdx-1 links histone H3-Lys-4 methylation to RNA polymerase II Elongation during activation of insulin transcription. *J Biol Chem*. 2005;280(43):36244–36253.
77. Sun BK, Deaton AM, Lee JT. A transient heterochromatic state in Xist preempts X inactivation choice without RNA stabilization. *Mol Cell*. 2006;21(5):617–628.
78. Dignam JD, Lebovitz RM, Roeder RG. Accurate transcription initiation by RNA polymerase II in a soluble extract from isolated mammalian nuclei. *Nucleic Acids Res*. 1983;11(5):1475–1489.
79. Evans-Molina C, Garmey JC, Ketchum RJ, Brayman K, Deng S, Mirmira RG. Glucose regulation of insulin gene transcription and pre–mRNA processing in human islets. *Diabetes*. 2007;56(3):827–835.
80. Iype T, et al. Mechanism of insulin gene regulation by the pancreatic transcription factor Pdx-1: application of pre-mRNA analysis and chromatin immunoprecipitation to assess formation of functional transcriptional complexes. *J Biol Chem*. 2005;280(17):16798–16807.
81. Deering TG, Ogihara T, Trace AP, Maier B, Mirmira RG. Methyltransferase Set7/9 maintains transcription and euchromatin structure at islet-enriched genes. *Diabetes*. 2009;58(1):185–193.